PHYSICAL REVIEW E **71**, 051503 (2005)

Nonlinear microstructure and rheology of semidilute colloidal suspensions of structureless particles

V. Zmievski and M. Grmela
CRASP, École Polytechnique de Montréal, Montréal H3C 3AV, Canada

M. Bousmina
Departement de Genie Chimique, Université Laval, Ste-Foy G1K 7P4, Canada

S. Dagréou
Laboratoire de Physico-Chimic des Polymères, Université de Pau et des Pays de l'AdourPau, France

(Received 27 January 2005; published 27 May 2005)

We investigate the influence of hydrodynamic and particle-particle interactions on the microstructure and rheological properties of semidilute colloidal suspensions of structureless particles. The time evolution is described in a mesoscopic setting in which the correlation tensor (second moment of the pair correlation function) is used as the microstructural state variable. Numerical solutions of the governing equations are then presented as linear and nonlinear responses of the suspensions to simple viscometric flows.

DOI: 10.1103/PhysRevE.71.051503 PACS number(s): 83.10.−y, 05.20.Dd, 05.70.Ln, 83.60.Df

I. INTRODUCTION

Let us consider a fluid composed of two types of microscopic particles: particles A and particles B. Let particles A not interact among themselves. They interact only with particles B which then interact among themselves. In this type of fluid the interactions A-B and B-B bring about interactions among particles A. These indirect A-A interactions are mediated by particles B. Now let particles B be much smaller than particles A so that the interactions A-B and B-B can be treated by means of classical hydrodynamics (by solving Stoke's problem). The induced A-A interactions are then called hydrodynamic interactions. The objective of this paper is to investigate fluids involving hydrodynamic interactions (HI suspensions). In particular, we contribute to answering the following two questions: (i) Can the Smoluchowski equation describing the time evolution of HI suspensions be reduced to a simpler equation if our interest is focused only on slower part of the time evolution? (ii) What are the linear and nonlinear responses of HI suspensions to imposed viscometric flows?

It is well known that the time evolution of HI suspensions can be formulated with the phase-space distribution function $\psi(\boldsymbol{r},\boldsymbol{R},\boldsymbol{V})$ serving as the variable characterizing the microstructure (the equation governing its time evolution is the Fokker-Planck type kinetic equation [1,2]) and also on a more macroscopic level on which the configuration-space distribution function $g(\boldsymbol{r},\boldsymbol{R})$ replaces $\psi(\boldsymbol{r},\boldsymbol{R},\boldsymbol{V})$ (the equation governing its time evolution is the Smoluchowski equation). By $\boldsymbol{r}$ we denote the position vector, $\boldsymbol{R}$ denotes the vector connecting two particles, and $\boldsymbol{V}$ is their relative velocity. The distribution functions ψ and g are related by $g(\boldsymbol{r},\boldsymbol{R}) = \int d\boldsymbol{V}\psi(\boldsymbol{r},\boldsymbol{R},\boldsymbol{V})$. The physics involved in the passage from the Fokker-Planck to the Smoluchowski description is the elimination of fast processes related to inertia of the suspended particles as they move through the fluid. The characteristic friction time τ_{fr} is a time scale of the Fokker-Planck equation. The characteristic relaxation time associated with the Smoluchowski equation is the self-diffusion time τ_S [see Eq. (24) in Sec. III]. In this paper we formulate a more macroscopic description on which $g(\boldsymbol{r},\boldsymbol{R})$, the state variable characterizing the microstructure in the Smoluchowski theory, is replaced by its second moment $\boldsymbol{m}(\boldsymbol{r},R)$ of $g(\boldsymbol{r},\boldsymbol{R})$ with respect to the unit vector $\boldsymbol{n}=\boldsymbol{R}/R$, $R=|\boldsymbol{R}|$—i.e., $m_{\alpha\beta}(\boldsymbol{r},R)=(R^2/4\pi)\int d\boldsymbol{n}n_\alpha n_\beta g(\boldsymbol{r},\boldsymbol{R})$. The idea behind the reduction $g(\boldsymbol{r},\boldsymbol{R})\rightarrow\boldsymbol{m}(\boldsymbol{r},R)$ is to keep only the largest time scale appearing in the spectrum of the self-diffusion process in the absence of overall flows. To describe states of HI suspensions by $\boldsymbol{m}$ has been suggested by Phan-Thien [3]. In this paper we follow his suggestion. We show how the hydrodynamic interactions are expressed in terms of $\boldsymbol{m}$ and solve the reduced Smoluchowski equation numerically. We recall that, in general, the advantage of introducing a reduced—i.e., a more macroscopic—description is in establishing a more direct link between the microscopic physics involved (in our case hydrodynamic interactions) and the macroscopic properties observed (in our case nonlinear rheology), and in simplifying the numerical calculations involved in the process of obtaining detailed solutions of the governing equations.

The second contribution of this paper is in deriving nonlinear rheology of HI suspensions. By the nonlinear rheology we mean nonlinear responses (both in the microstructure and the stresses) to imposed simple shear and elongation flows. Our limitation to time scales implies that responses to rapidly varying (with the time scales that are smaller than the ones kept in the governing equations) external forces are outside the scope of our investigation. We compare our results with experimental data [4], direct numerical simulations (Stokesian dynamics of suspended particles [5]), and previous attempts to solve approximatively the Smoluchowski equation [6–10] (see also Sec. V). We also show that the linear rheology (linear response to the oscillatory shear flow) implied by our results agrees with the investigations reported in [11–13].

1539-3755/2005/71(5)/051503(18)/$23.00

To appreciate the new challenges that we meet in this paper, we compare briefly our investigation with the same type of investigation conducted in the context of dilute polymeric suspensions [14]. The state variable describing the internal structure of dilute polymeric suspensions is often chosen to be also the pair correlation function $g(\boldsymbol{R})$ and the equation governing its time evolution resembles the Smoluchowski equation for the HI suspensions. The essential difference between suspensions of structureless particles and dilute polymeric suspensions is in the physical interpretation of $g(\boldsymbol{R})$ and in the interactions. In particle suspensions the correlation function $g(\boldsymbol{R})$ characterizes interparticle correlations ($\boldsymbol{R}$ is in this case the vector connecting two suspended particles), and in dilute polymeric suspensions $g(\boldsymbol{R})$ characterizes intramolecular correlations ($\boldsymbol{R}$ is in this context the end-to-end vector of a single molecule). As for the interactions, the interparticle interactions, determining macroscopic behavior of particle suspensions, vanish as $\boldsymbol{R}\to\infty$. This is true both for the direct interaction (generated by an interparticle potential) and also for hydrodynamic interactions (that are not generated by a potential). Consequently, two suspended particles become uncorrelated when they are far apart which implies that $g(\boldsymbol{R})$ does not decay to zero as $\boldsymbol{R}\to\infty$. On the other hand, the intramolecular interactions, determining the macroscopic behavior of dilute polymeric suspensions, tend to infinity as $\boldsymbol{R}\to\infty$. This then means that $g(\boldsymbol{R})$ tends rapidly to zero as $\boldsymbol{R}\to\infty$. The asymptotic behavior of $g(\boldsymbol{R})$ in HI suspensions is a source of anomalies [like divergence of moments of $g(\boldsymbol{R})$] that render many of the methods (e.g., stochastic dynamic simulation or reductions) developed for solving the Smoluchowski equations corresponding to polymeric suspensions inapplicable to the HI suspensions. For example, let us consider the method of reduction. For this method to work, it is necessary that the time evolution can be split into slow and fast. The existence of such a scale separation is seen in the spectrum of the operator appearing in the dissipative part (i.e., the part that does not involve the overall flow) of the right-hand side of the Smoluchowski equation (note that it is indeed a linear operator). If the spectrum is, in the vicinity of zero, discrete and sufficiently separated from the rest of the spectrum, then the scale separation exists and the eigenfunctions corresponding to the discrete eigenvalues provide an appropriate basis for describing slow time evolution. In the case of polymeric solutions, the Smoluchowski equation has such a property and the eigenfunctions corresponding to the discrete eigenvalues are well approximated by polynomial functions [15]. This is the main reason why the second moment [i.e., $\int d\boldsymbol{R}\boldsymbol{R}\boldsymbol{R}g(\boldsymbol{R})$] serves as an appropriate state variable in reduced theories. The Smoluchowski equation for HI suspensions does not have this property; moreover, the second moment does not even exist [due to the fact that $g(\boldsymbol{R})\to\text{const}$ as $\boldsymbol{R}\to\infty$]. Our method of reducing the Smoluchowski equation for HI suspensions is based on the observation that if we consider the dissipative operator as a composition of two operators, one acting only on the angular dependence and the other on the radial dependence of $g(\boldsymbol{R})$, then the angular part still keeps the properties guaranteeing the scale separation. The radial dependence is then treated separately by applying an appropriately adapted finite-element method.

The most well-known example of HI suspensions is a semidilute suspension of rigid spheres of diameter a ($a \ll L$, where L is the dimension of the system). In this paper we assume that the suspensions are incompressible, isothermal, and homogeneous. The assumption of homogeneity (i.e., the assumption that the correlation function is independent of the position vector $\boldsymbol{r}$ and the volume fraction of the suspended particles is absent in the set of state variables) prevents us from investigating the experimentally observed flow-induced diffusion of the suspended particles. We intend to return to this point in a future publication

This paper is organized as follows. In Sec. II we present the Smoluchowski equation for HI suspensions. We make no attempt to discuss its derivation from microhydrodynamics. Instead, our attention is focused on the macroscopic behavior implied by it. In other words, we take the Smoluchowski equation as given and investigate (from both the mathematical and physical points of view) its solutions. In Sec. III, we investigate asymptotic (as $t\to\infty$) solutions and the related problem of the compatibility of the time evolution with thermodynamics. This investigation gives us also an expression for the extra stress tensor. In Sec. IV we reduce the Smoluchowski equation to a moment equation. We discuss its physical content and, in Sec. V, we solve it numerically. The solutions are then presented as responses of the microstructure and the stresses to imposed viscometric flows. Our results allow us to investigate the influence of hydrodynamic and various interparticle interactions on the microstructure and rheology.

II. SMOLUCHOWSKI EQUATION

Following Smoluchowski [16], we choose to describe the microstructure of suspensions by the pair correlation function $g(\boldsymbol{R})$, where the vector $\boldsymbol{R}$ is the vector connecting two suspended particles. The equations governing its time evolution is the Smoluchowski equation

$$\frac{\partial g}{\partial t} = -\frac{\partial}{\partial R_\alpha}\left(gR_\beta\frac{\partial v_\alpha}{\partial r_\beta}\right) + \frac{\partial}{\partial R_\gamma}(g\lambda_{\gamma\alpha\beta}D_{\alpha\beta}) + \frac{\partial}{\partial R_\alpha}\left(g\Lambda_{\alpha\beta}\frac{\partial}{\partial R_\beta}(U + k_BT\ln g)\right). \tag{1}$$

Here and throughout the text we use the summation convention (summation over repeated Greek indices). By $\boldsymbol{v}(\boldsymbol{r})$, we denote the overall velocity of the suspension, $\boldsymbol{r}$ denotes the position vector, $\boldsymbol{D}$ denotes the rate of a strain tensor,

$$D_{\alpha\beta} = \frac{1}{2}\left(\frac{\partial v_\alpha}{\partial r_\beta} + \frac{\partial v_\beta}{\partial r_\alpha}\right),$$

and the tensors $\boldsymbol{\Lambda}$ and $\boldsymbol{\lambda}$ are kinetic coefficients which are functions of $\boldsymbol{R}$, radius of particles, a, and density of particles, n_p, or equivalently volume fraction $\phi=(4/3)\pi n_p a^3$.

Without lost of generality the functions $\boldsymbol{\Lambda}(\boldsymbol{R},\phi)$, $\boldsymbol{\lambda}(\boldsymbol{R},\phi)$ can be written in the following form:

$$\Lambda_{\alpha\beta} = \frac{k_BT}{3\pi\eta_0 a}\left[\sigma_1(R/a,\phi)\frac{R_\alpha R_\beta}{R^2} + \sigma_2(R/a,\phi)\left(\delta_{\alpha\beta} - \frac{R_\alpha R_\beta}{R^2}\right)\right], \tag{2}$$

$$\lambda_{\alpha\beta\gamma} = \left[\mu_1(R/a,\phi)\frac{R_\alpha R_\beta}{R^2} + \mu_2(R/a,\phi)\left(\delta_{\alpha\beta} - \frac{R_\alpha R_\beta}{R^2}\right)\right] R_\gamma. \tag{3}$$

Regarding the tensor $\boldsymbol{\lambda}$, we take into account the fact that $\boldsymbol{\lambda}$ enters the time evolution equation (1) as well as the stress tensor (see Sec. III A below) only in symmetrized and traceless form, $\mathring{\lambda}$, with respect to last two indices:

$$\mathring{\lambda}_{\gamma\alpha\beta} = \frac{1}{2}\left(\lambda_{\gamma\alpha\beta} + \lambda_{\gamma\alpha\beta} - \frac{2}{3}\delta_{\alpha\beta}\lambda_{\gamma\sigma\sigma}\right).$$

Below, we shall continue to use the symbol ○ to indicate symmetrized and traceless part of second-order tensors.

We have introduced the dimensional factor $k_BT/3\pi\eta_0 a$ in $\boldsymbol{\Lambda}$, because $\boldsymbol{\Lambda}$ plays the role of an *anisotropic* diffusion matrix describing a self-diffusion of particles in the presence of hydrodynamic interactions; a is the diameter of the sphere, η_0 is the viscosity coefficient of the Newtonian fluid in which the spheres are suspended, k_B is the Boltzmann constant, and T is the temperature (assumed to be constant).

Specific features of hydrodynamic interactions are expressed in the coefficients $\sigma_1(R/a,\phi)$, $\sigma_2(R/a,\phi)$, $\mu_1(R/a,\phi)$, and $\mu_2(R/a,\phi)$. The functions σ_1 and σ_2 must be non- negative (in order to guarantee the non-negativeness of the diffusion matrix $\boldsymbol{\Lambda}$—see Sec. III), but otherwise, they can be seen as parameters in the governing equations that can be adjusted to fit experimental data. In our computations in Sec. V we consider only zeroth-order terms in ϕ (we limit ourselves only to binary interactions) and we use expressions of Batchelor and Green [28] (see Appendix A).

In order to be able to see how the hydrodynamic interactions influence the evolution of the microstructure and the rheology, we shall also consider suspensions with no hydrodynamic interactions. In such suspensions the surrounding fluid imposes only a drag force on single particles and particles interact as rigid spheres—i.e., through hard-core interactions. In Eq. (1) this corresponds to the choice $\boldsymbol{\lambda}=0$ and $\boldsymbol{\Lambda}=\boldsymbol{\delta}k_BT/(3\pi\eta_0 a)$ $(\sigma_1=\sigma_2=1)$.

By $U(\boldsymbol{R})$ we denote the total two-particle potential energy due to the particle-particle interactions. It is a sum

$$U = U_{\mathrm{HC}} + U_{\mathrm{nl}}$$

of the hard core potential U_{HC},

$$U_{\mathrm{HC}}(R) = \begin{cases} 0, & \text{for } R > 2a, \\ \infty, & \text{for } R \leqslant 2a. \end{cases} \tag{4}$$

and a nonlocal potential U_{nl} arising due to long-range (i.e., beyond the intermolecule scale) interactions such as electrostatic forces or some self-consistent effective potential taking into account multiparticle interactions (in with case it may depend on g). In this paper we shall take into account the hard-core potential by applying specific boundary condition at the surface of the particle, $R=2a$ (see the end of this section). Only the nonlocal part U_{nl} of the potential energy is kept hereafter in the Smoluchowski equation (1). In our calculations we shall choose U_{nl} to be the repelling part of the Lennard-Jones potential,

$$U_{\mathrm{nl}}(R) = \frac{\epsilon}{R^{12}}, \quad \text{for } R \geqslant 2a, \tag{5}$$

where ϵ is some positive constant.

The usual way to arrive at Eq. (1) (see, e.g., [17,18]) is to select one particle in the suspension, analyze all the forces acting on it, write the Newton equations, neglect the inertia, and finally write the corresponding Liouville (continuity) equation which then becomes Eq. (1). The forces acting on the selected particle are the force due to the direct particle-particle interactions (i.e., the forces generated by the potential U), the Brownian force (the force generated by $k_BT \ln g$), and the force mediated by the fluid due to the hydrodynamic interactions [expressed in Eq. (1) in the terms involving the tensors $\boldsymbol{\Lambda}$ and $\boldsymbol{\lambda}$]. From the simplifying assumptions made in the process of the derivation of Eq. (1) we may expect that the suspensions are rather dilute, isothermal, monodisperse, homogeneous, and incompressible suspensions of rigid spheres in Newtonian fluids. The spheres are all identical and their radius a is much smaller than the characteristic linear size L of the fluid container. The concentration of the suspension is limited mainly by considering only binary hydrodynamic interactions. Another way to estimate the range of applicability of the Smoluchowski equation is to derive its consequences for the macroscopic behavior. Our investigation proceeds in the latter direction.

Equation (1) has to be supplemented by appropriate boundary conditions. For the far-field limit $R\to\infty$, we assume that the correlation function g tends to n_p^2 (i.e., to the uniform distribution),

$$g(R\to\infty)\to n_p^2, \tag{6}$$

where n_p is the number density of suspended particles, assumed to be a constant.

Another boundary is the surface of the particle, $R\to 2a$. For this boundary we adopt the boundary condition introduced by Batchelor [17]. The flux, defined by the Smoluchowski equation, through the boundary, in the direction perpendicular to it, vanishes—i.e., $n_\alpha J_\alpha|_{R=2a}=0$, where $n_\alpha = R_\alpha/R$ and

$$J_\alpha = \left(gR_\beta\frac{\partial v_\alpha}{\partial r_\beta} + g\lambda_{\alpha\beta\gamma}\boldsymbol{D}_{\beta\gamma}\right) + g_{\mathrm{eq}}\Lambda_{\alpha\beta}\frac{\partial}{\partial R_\beta}\frac{g}{g_{\mathrm{eq}}}, \tag{7}$$

g_{eq} is the equilibrium correlation function defined as

$$g_{\mathrm{eq}} = \exp\left(-\frac{U_{\mathrm{nl}}}{k_BT}\right). \tag{8}$$

Written explicitly, this condition takes the form

$$\sigma_1(2a)g_{\mathrm{eq}}(2a)\left.\left[n_\beta\frac{\partial}{\partial R_\beta}\frac{g}{g_{\mathrm{eq}}}\right]\right|_{R=2a} + 2ag(2a\boldsymbol{n}) \times(\mu_1(2a)-1)\boldsymbol{nn}:\boldsymbol{D}=0. \tag{9}$$

We note that due to the asymptotic behavior of $\mu_1(R)$ ($\mu_1\to 1$, when $R\to 2a$; see Appendix A), the second term in Eq. (9) vanishes. In the absence of hydrodynamic interactions this term is different from zero and plays the role of the force driving the correlation function g out of equilibrium.

We also note that in the presence of hydrodynamic interactions the function σ_1 vanishes on the boundary $R=2a$ as well (see Appendix A). In spite of it, Eq. (9) remains to be a meaningful condition (both in the presence and in the absence of hydrodynamic interactions) selecting a unique solution to our initial boundary value problem [19].

In this paper we shall not contribute in any way to the clarification of the relation between Eq. (1) and the microhydrodynamic viewpoint of suspensions. Our objective is to take Eq. (1) as an equation representing a given mesoscopic theory and look towards its more macroscopic consequences. In particular, we shall investigate the compatibility of Eq. (1) with thermodynamics, derive a reduced model of Eq. (1), and derive the nonlinear rheology implied by it.

III. DYNAMICS AND THERMODYNAMICS OF HI SUSPENSIONS

In the sequel we want to consider rheological consequences of Eq. (1). We thus have to extend the set of state variables by adopting into it the average overall momentum $\boldsymbol{u}(\boldsymbol{r})$. The time evolution equation (1) extends to

$$\frac{\partial u_\alpha}{\partial t} = -\frac{\partial}{\partial r_\gamma}(u_\gamma v_\alpha + \delta_{\gamma\alpha} p + \sigma_{\alpha\gamma}), \tag{10}$$

$$\frac{\partial g}{\partial t} = -\frac{\partial}{\partial R_\alpha}\left(g R_\beta \frac{\partial v_\alpha}{\partial r_\beta}\right) + \frac{\partial}{\partial R_\gamma}(g \lambda_{\gamma\alpha\beta} D_{\alpha\beta}) + \frac{\partial}{\partial R_\alpha} g_{\mathrm{eq}} \Lambda_{\alpha\beta} \frac{\partial}{\partial R_\beta} \frac{g}{g_{\mathrm{eq}}}. \tag{11}$$

Equation (10) is the standard local momentum conservation law, $\boldsymbol{v}=\boldsymbol{u}/\rho$, ρ is the overall mass density of the suspension (a constant), p is the hydrostatic pressure (determined by the incompressibility requirement), and $\boldsymbol{\sigma}$ is the extra stress tensor that remains to be specified.

A. Extra stress tensor

In order to find the expression for the extra stress tensor, we can either turn to microhydrodynamics (see, e.g., [17,20]) and analyze forces acting on a surface element placed inside the suspension, or we can turn to macroscopic consequences of Eqs. (10) and (11) [i.e., solutions of Eqs. (10) and (11)] and to their comparison with results of macroscopic observations. Since we have already decided not to look into the microscopic basis of the Smoluchowski equation (11), we naturally take the second route.

The macroscopic observation that we shall require to be reproduced in solutions of Eqs. (10) and (11) is the approach to equilibrium and the applicability of classical thermodynamics to describe the behavior of suspensions at the equilibrium. Let $\Phi(\boldsymbol{u},g)$ be the free energy of the suspension. In a system under consideration it is given by

$$\Phi = \int \mathrm{d}\boldsymbol{r}\left(\frac{u^2}{2\rho} + \int \mathrm{d}\boldsymbol{R}\, g(U_{\mathrm{nl}} + k_B T \ln g)\right). \tag{12}$$

We recall that the free energy equals the entropy mines the energy multiplied by the temperature T (a constant in this paper). For the entropy we take the Boltzmann expression. The energy is a sum of the kinetic energy of the overall flow and the potential energy $\langle U_{\mathrm{nl}}\rangle = \int d\boldsymbol{R} g U_{\mathrm{nl}}$ arising due to the presence of the suspended particles. As we discussed above we have excluded the singular hard-core interaction energy U_{HC} from the free energy.

The requirement that the time evolution is compatible with thermodynamics implies

$$\frac{\mathrm{d}\Phi}{\mathrm{d}t} \leqslant 0. \tag{13}$$

As the time $t\to\infty$ the free energy $\Phi(\boldsymbol{u},g)$ reaches its minimum. The states at which Φ reaches its minima are called equilibrium states $(u_{\mathrm{eq}}, g_{\mathrm{eq}})$. As we see immediately from Eq. (12), it is the state at which no flow takes place (i.e., $\boldsymbol{u}=\boldsymbol{0}$) and $U_{\mathrm{nl}}=\ln g_{\mathrm{eq}}$, where g_{eq} is the equilibrium pair correlation function. When $U_{\mathrm{nl}}=0$—i.e., when the suspended particles interact only via the hard-core potential—then $g_{\mathrm{eq}}=1$.

Following [24], we shall express the compatibility of dynamics with thermodynamics in a somewhat stronger requirement. In order to formulate it we need an additional notation. Let $z:=(\boldsymbol{u},g)$ and Eqs. (10) and (11) be formally written as

$$\frac{dz}{dt} = F(z). \tag{14}$$

The right-hand side of Eqs. (10) and (11)—i.e., $F(z)$—is, moreover, written as a sum of the time reversible part $F^{(\mathrm{rev})} \times (z)$ and the time irreversible part $F^{(\mathrm{irrev})}(z)$:

$$\frac{dz}{dt} = F^{(\mathrm{rev})}(z) + F^{(\mathrm{irrev})}(z), \tag{15}$$

with

$$F^{(\mathrm{rev})}\begin{pmatrix}\mathbf{u}\\ g\end{pmatrix} = \begin{pmatrix} -\dfrac{\partial}{\partial r_\gamma}(u_\gamma \Phi_{u_\alpha} + \delta_{\gamma\alpha} p + \sigma^{(\mathrm{rev})}_{\alpha\gamma}) \\ -\dfrac{\partial}{\partial R_\alpha}\left(g R_\beta \dfrac{\partial \Phi_{u_\alpha}}{\partial r_\beta}\right) + \dfrac{\partial}{\partial R_\gamma}(g \lambda_{\gamma\alpha\beta} D_{\alpha\beta}) \end{pmatrix},$$

$$F^{(\mathrm{irrev})}\begin{pmatrix}\mathbf{u}\\ g\end{pmatrix} = \begin{pmatrix} -\dfrac{\partial}{\partial r_\gamma}\sigma^{(\mathrm{irrev})}_{\alpha\gamma} \\ \dfrac{\partial}{\partial R_\alpha}\left(g \Lambda_{\alpha\beta} \dfrac{\partial}{\partial R_\beta}\Phi_g\right) \end{pmatrix}, \tag{16}$$

where

$$D_{\alpha\beta} = \frac{1}{2}\left(\frac{\partial}{\partial r_\alpha}\Phi_{u_\beta} + \frac{\partial}{\partial r_\beta}\Phi_{u_\alpha}\right)$$

and Φ_g and $\Phi_{\boldsymbol{u}}$ denote variational derivatives of the free energy functional (12) with respect to the corresponding function—i.e., $\Phi_g = (\delta\Phi/\delta g)$ and $\Phi_{\boldsymbol{u}} = (\delta\Phi/\delta\boldsymbol{u})$.

We recognize the time reversible and irreversible parts of the vector field by evenness and oddness with respect to time inversion operator $\mathcal{I}$; $\mathcal{I}(\boldsymbol{u},g) = (-\boldsymbol{u},g)$. We thus have

$F^{(\mathrm{rev})}(\mathcal{I}z)=-F^{(\mathrm{rev})}(z)$ and $F^{(\mathrm{irrev})}(\mathcal{I}z)=F^{(\mathrm{irrev})}(z)$. We are also splitting the stress tensor into the time reversible and irreversible parts,

$$\boldsymbol{\sigma}(z)=\boldsymbol{\sigma}^{(\mathrm{rev})}(z)+\boldsymbol{\sigma}^{(\mathrm{irrev})}(z),$$

with $\boldsymbol{\sigma}^{(\mathrm{rev})}(\mathcal{I}z)=-\boldsymbol{\sigma}^{(\mathrm{rev})}(z)$ and $\boldsymbol{\sigma}^{(\mathrm{irrev})}(\mathcal{I}z)=\boldsymbol{\sigma}^{(\mathrm{irrev})}(z)$.

Now, we are prepared to formulate the stronger requirement of the compatibility of dynamics with thermodynamics. Instead of Eq. (13), we shall require

$$\left(\frac{d\Phi}{dt}\right)_{(\mathrm{rev})}=0, \tag{17}$$

$$\left(\frac{d\Phi}{dt}\right)_{(\mathrm{irrev})}\leqslant 0, \tag{18}$$

where the subscripts (rev) respectively (irrev) describe the reversible and irreversible parts, respectively, of the time evolution equation. In other words, Eqs. (17) and (18) mean that the time-reversible part of the time evolution is nondissipative and the time-irreversible part is dissipative. What are the physical arguments with which we can support the requirements (17) and (18)?

First, we note that in the particular case when the time reversible evolution constitutes the complete time evolution (as it is, for example, in the case of the time evolution governed by the Liouville equation corresponding to the Hamilton dynamics of classical particles), the time-reversible part is indeed nondissipative. This is a well-known fact. The requirements (17) and (18) can be thus seen as an extension of the association of time reversibility with nondissipativity known from the microscopic time evolution to the mesoscopic time evolution where the reversible time evolution represents only a part of the complete time evolution. The second argument supporting Eqs. (17) and (18) comes from its association with the Onsager-Casimir relations. If we linearize Eq. (14) about equilibrium states (i.e., states at which Φ attains its minimum) and use the Onsager-Casimir relations (i.e., the statement that the linearized part of the reversible and irreversible parts, respectively, of F, is skew-adjoint and self-adjoint, respectively, with respect to the inner product involving the second derivative of the free energy as the weight function) then, as we immediately see, the linearized version of Eqs. (17) and (18) is a consequence of the Onsager-Casimir relations. The third argument in favor of Eqs. (17) and (18) comes from its association with the GENERIC formalism (see [25] and references cited therein), which is a structure extracted as a common structure of many well established (i.e., well tested with results of experimental observations) mesoscopic dynamical theories describing a time evolution that is compatible with thermodynamics. This structure, which can also be seen as a nonlinear extension of the Onsager-Casimir relation (see [26]), implies Eqs. (17) and (18).

As for the irreversible part of the extra stress tensor, we shall choose the standard Navier-Stokes constitutive relation with the overall fluid viscosity containing Einstein contribution [27] due to one-particle hydrodynamic self-interactions:

$$\sigma^{(\mathrm{irrev})}_{\alpha\beta}=-\eta_0\left(1+\frac{5}{2}\phi\right)D_{\alpha\gamma}. \tag{19}$$

We see that the viscosity depends linearly on the volume fraction ϕ of suspended particles, $\phi=(4/3)n_p a^3$.

It is easy to verify that

$$\left(\frac{d\Phi}{dt}\right)_{(\mathrm{irrev})}=-\frac{1}{2}D_{\alpha\beta}\eta_0\left(1+\frac{5}{2}\phi\right)D_{\alpha\beta}-\int d\boldsymbol{R}\left(\frac{\partial}{\partial R_\alpha}\Phi_g\right)g\Lambda_{\alpha\beta}\left(\frac{\partial}{\partial R_\beta}\Phi_g\right)\leqslant 0, \tag{20}$$

and thus Eq. (18) holds provided $\boldsymbol{\Lambda}$ is a positive definite tensor and η_0 is a positive coefficient.

Next, we find $\boldsymbol{\sigma}^{(\mathrm{rev})}$ from the requirement (17). A direct calculation of $(d\Phi/dt)_{(\mathrm{rev})}$ (see [24] for more details) leads us to

$$\sigma^{(\mathrm{rev})}_{\alpha\beta}=-\int \mathrm{d}\boldsymbol{R}g\left(R_\alpha\frac{\partial}{\partial R_\beta}-\frac{1}{3}\delta_{\alpha\beta}R_\gamma\frac{\partial}{\partial R_\beta}-\mathring{\lambda}_{\gamma\alpha\beta}\frac{\partial}{\partial R_\gamma}\right)\Phi_g. \tag{21}$$

The inequality (13), which is now guaranteed provided the extra stress tensor is given by Eqs. (19) and (21), means that the free energy Φ plays in the time evolution governed by Eqs. (10) and (11) the role of a Lyapunov function. This Lyapunov function guarantees the approach (as $t\to\infty$) to the equilibrium sates that minimize the free energy. We thus conclude by saying that Eq. (1) is compatible with equilibrium thermodynamics provided the extra stress tensor is given by the sum of the irreversible, Eq. (19), and the reversible, Eq. (21), parts, $\eta_0>0$, and $\boldsymbol{\Lambda}$ is a positive-definite tensor.

Finally, collecting all contributions to the extra stress tensor and taking into account the boundary conditions (6), we arrive at

$$\sigma_{\alpha\beta}=\sigma^{\mathrm{hydr}}_{\alpha\beta}+\sigma^{\mathrm{DI}}_{\alpha\beta}+\sigma^{\mathrm{HI}}_{\alpha\beta}, \tag{22}$$

where

$$\sigma^{\mathrm{hydr}}_{\alpha\beta}=-\eta_0\left(1+\frac{5}{2}\phi\right), \tag{23}$$

$$\sigma^{\mathrm{DI}}_{\alpha\beta}=2\int_{\mathrm{S}_2}\mathrm{d}\boldsymbol{n}\left(n_\alpha n_\beta-\frac{1}{3}\delta_{\alpha\beta}\right)\Delta g(2a\boldsymbol{n})-\int \mathrm{d}\boldsymbol{R}R\frac{\partial U_{\mathrm{nl}}}{\partial R}\times\left(n_\alpha n_\beta-\frac{1}{3}\delta_{\alpha\beta}\right)\Delta g(\boldsymbol{R}), \tag{24}$$

$$\sigma^{\mathrm{HI}}_{\alpha\beta}=-2\mu_1(2a)\int_{\mathrm{S}_2}\mathrm{d}\boldsymbol{n}\left(n_\alpha n_\beta-\frac{1}{3}\delta_{\alpha\beta}\right)\Delta g(2a\mathbf{n})-\int \mathrm{d}\boldsymbol{R}\left[3(\mu_1-\mu_2)+R\frac{\partial\mu_1}{\partial R}+\mu_1 R\frac{\partial U_{\mathrm{nl}}}{\partial R}\right]\times\left(n_\alpha n_\beta-\frac{1}{3}\delta_{\alpha\beta}\right)\Delta g(\boldsymbol{R}). \tag{25}$$

By the symbol $\Delta g=g-g_{\mathrm{eq}}$ we denote a deviation from equilibrium of the correlation function. The integration in Eqs. (24) and (25) is over the two-dimensional unit sphere $\mathbb{S}_2$.

The first term on the right-hand side of Eq. (22), $\boldsymbol{\sigma}^{\mathrm{hydr}}$, is a contribution from the Newtonian fluid in which particles are suspended. The second term, σ^{DI}, comes from the direct interactions including the hard core [first term in Eq. (24)] and a long-range soft tail potential U_{nl}. The third term in Eq. (22), $\boldsymbol{\sigma}^{\mathrm{HI}}$, is a contribution arising due to hydrodynamic interactions.

We note that the part $\boldsymbol{\sigma}_p = \boldsymbol{\sigma}^{\mathrm{HI}} + \boldsymbol{\sigma}^{\mathrm{DI}}$ of the extra stress tensor that arises due to the presence of suspended particles is traceless. We also note that due to the near-field asymptotic behavior of the function $\mu_1(R)$ [$\mu_1 \to 1$, as $R \to 2$; see Eq. (A7)] the local part of the extra stress tensor σ_p (i.e., the sum of the first term in $\boldsymbol{\sigma}^{\mathrm{HI}}$ and $\boldsymbol{\sigma}^{\mathrm{DI}}$) vanishes. This is a consequence of the lubrification approximation used in the derivation of the near-field asymptotics of the coefficients μ_1 and μ_2 [28]. However, when we consider the suspension of hard spheres without hydrodynamic interactions, this local term is different from zero and provides the only contribution to $\boldsymbol{\sigma}_p$.

It is satisfying to see that the stress tensor (29), derived above from the requirement of the compatibility of dynamics with thermodynamics, coincides (in the case $U_{\mathrm{nl}}=0$) with the expression obtained by Batchelor [17] in the setting of microhydrodynamics.

B. Dimensionless formulation

In this subsection we transform the governing equations introduced above to dimensionless form. We begin by introducing the dimensionless time $t \to t/\tau_{\mathrm{S}}$, where τ_{S} is the characteristic relaxation time associated with the Smoluchowski equation (11):

$$\tau_{\mathrm{S}} = \frac{6\pi\eta_0 a^3}{k_B T}. \tag{26}$$

Another characteristic time arising naturally in Eqs. (10) and (11) is the hydrodynamic time τ_{hyd} defined via characteristic scalar rate of strain $\dot{\gamma}$ [for constant tensor $\boldsymbol{D}$ the scalar strain rate is defined as $\dot{\gamma} = (D_{\alpha\beta} D_{\beta\alpha})^{1/2}$],

$$\tau_{\mathrm{hyd}} = \dot{\gamma}^{-1}. \tag{27}$$

We introduce dimensionless position coordinates $\boldsymbol{r}$ and $\boldsymbol{R}$ as follows:

$$\boldsymbol{r} \to \boldsymbol{r}/a, \boldsymbol{R} \to \boldsymbol{R}/a.$$

The overall momentum $\boldsymbol{u} \to \boldsymbol{u}/u_0$, where the characteristic velocity u_0 is defined by

$$u_0 = \rho a/\tau_{\mathrm{hyd}}.$$

The dimensionless form of the rest of the variables entering the governing equations (10) and (11) is given by

$$g \to \frac{g}{n_p^2}, \quad p \to \frac{\tau_{\mathrm{hyd}}^2}{\rho a^2} p, \quad \sigma_{\alpha\gamma} \to \frac{1}{\eta_0 \dot{\gamma}} \sigma_{\alpha\gamma},$$

$$U_{\mathrm{nl}} \to \frac{1}{k_B T} U_{\mathrm{nl}}, \quad \Lambda_{\alpha\beta} \to \frac{3\pi\eta_0 a}{k_B T} \Lambda_{\alpha\gamma}, \quad \lambda_{\alpha\beta\gamma} \to \frac{1}{a} \lambda_{\alpha\beta\gamma}.$$

Here n_p is the number density of the suspended particles.

The resulting dimensionless form of Eqs. (10), (11), (22), and (21), is now

$$\frac{\partial u_\alpha}{\partial t} = -\mathrm{Pe} \frac{\partial}{\partial r_\gamma} \left(u_\gamma v_\alpha + \delta_{\gamma\alpha} p + \frac{1}{\mathrm{Re}} \sigma_{\alpha\gamma} \right),$$

$$\frac{\partial g}{\partial t} = -\mathrm{Pe} \frac{\partial}{\partial r_\gamma} v_\gamma g - \mathrm{Pe} \frac{\partial}{\partial R_\alpha} R_\beta \frac{\partial v_\alpha}{\partial r_\beta} \Delta g + \mathrm{Pe} \frac{\partial}{\partial R_\gamma} g \lambda_{\gamma\alpha\beta} \boldsymbol{D}_{\alpha\beta} + \frac{\partial}{\partial R_\alpha} g_{\mathrm{eq}} \Lambda_{\alpha\beta} \frac{\partial}{\partial R_\beta} \frac{g}{g_{eq}} \tag{28}$$

and the extra stress tensor

$$\sigma_{\alpha\beta} = -\left(1 + \frac{5}{2}\phi\right) D_{\alpha\gamma} - \frac{27}{8\pi} \frac{\phi^2}{\mathrm{Pe}} \Bigg\{ 2 \int_{\mathbb{S}_2} \mathrm{d}\boldsymbol{n} \left(n_\alpha n_\beta - \frac{1}{3}\delta_{\alpha\beta} \right) \times [1 - \mu_1(2)] \Delta g(2n) - \int \mathrm{d}\boldsymbol{R} \left[3(\mu_1 - \mu_2) + R \frac{\partial \mu_1}{\partial R} + (1 - \mu_1) R \frac{\partial U_{\mathrm{nl}}}{\partial R} \right] \left(n_\alpha n_\beta - \frac{1}{3}\delta_{\alpha\beta} \right) \Delta g(\boldsymbol{R}) \Bigg\}. \tag{29}$$

Here $\phi = (4/3) n_p \pi a^3$ is the volume fraction of particles in a fluid.

In the above equations we have introduced two well-known dimensionless constants: the Reynolds number, Re, and the Péclet number, Pe, defined as

$$\mathrm{Re} = \frac{u_0 a}{\eta_0} = \frac{\rho a^2 \dot{\gamma}}{\eta_0},$$

$$\mathrm{Pe} = \frac{\tau_{\mathrm{S}}}{\tau_{\mathrm{hyd}}} = \dot{\gamma} \frac{6\pi\eta_0 a^3}{k_B T}.$$

The Péclet number is a ratio of mesoscopic (associated with the time evolution of the internal structure) and macroscopic (hydrodynamic) time scales. In the Smoluchowski equation (28) the Péclet number can be regarded as a scalar parameter measuring strength of the hydrodynamic flow.

IV. MOMENT MODEL OF THE SMOLUCHOWSKI EQUATION (MS EQUATION)

The possibility that Eq. (28) can be solved analytically in a closed form is quite remote. We turn therefore to numerical methods and/or to their appropriate combinations with analytical methods. We can, at least in principle, take a direct numerical approach to finding solutions of Eq. (28). In order to avoid very cumbersome reformulations (discretizations) of Eq. (28) needed on this route, we shall follow another route on which the search for solutions of Eqs. (28) takes a physical meaning. We begin by realizing that in order to derive a nonlinear rheology of suspensions (the main objective of this paper) we do not need all the details of solutions of the Smoluchowski equation. We need, as we shall argue below, only information about the slow part of the time evolution. The question then arises as to whether we can identify an equation, which we expect to be simpler than Eq. (28) (simpler in the sense of finding numerically its solution), describing just the slow time evolution. We shall now proceed to find such equation.

In order to identify the slow state variables we need to recognize in the Smoluchowski equation a hierarchy of characteristic relaxation times. Such a hierarchy is revealed if we look at the set of moments of the orientation vectors $\boldsymbol{n} = \boldsymbol{R}/R$:

$$M^{[k]}_{\alpha_1\cdots\alpha_n}(R) = \frac{R^2}{4\pi}\int \mathrm{d}\boldsymbol{n}\, g(\boldsymbol{R})\, n_{\alpha_1}\cdots n_{\alpha_k},$$

where k indicates the order of the moment. By averaging Eq. (28) with corresponding weights we construct the following hierarchy of equations governing the time evolution of the moments $\boldsymbol{M}^{[k]}$ (k are even and positive integers):

$$\frac{\partial \boldsymbol{M}^{[k]}}{\partial t} = \mathrm{Pe}\Bigg\{ kS_k\boldsymbol{\omega}\cdot\boldsymbol{M}^{[k]} + \frac{\partial}{\partial R}R(\mu_1-1)\boldsymbol{D}{:}\boldsymbol{M}^{[k+2]} + k(1-\mu_2) \times\left(S_k\boldsymbol{D}\cdot\boldsymbol{M}^{[k]} - \boldsymbol{D}{:}\boldsymbol{M}^{[k+2]}\right)\Bigg\} + \frac{\partial}{\partial R}\sigma_1\hat{g}_{\mathrm{eq}}\frac{\partial}{\partial R}\frac{\boldsymbol{M}^{[k]}}{\hat{g}_{\mathrm{eq}}} - k(k+1)\frac{\sigma_2}{R^2}\left(\boldsymbol{M}^{[k]} - \frac{k-1}{k+1}S_k(\delta\boldsymbol{M}^{[k-2]})\right). \qquad (30)$$

Here $k=0,2,4,\ldots$, $\hat{g}_{\mathrm{eq}}$ denotes the equilibrium radial pair correlation function $\hat{g}_{\mathrm{eq}} = R^2 g_{\mathrm{eq}}$, the tensor $\boldsymbol{\omega}$ is the flow vorticity tensor,

$$\omega_{\alpha\beta} = \frac{1}{2}\left(\frac{\partial v_\alpha}{\partial r_\beta} - \frac{\partial v_\beta}{\partial r_\alpha}\right),$$

and the symbol S_k denotes the symmetrization operation,

$$(S_kA)_{\alpha_1\cdots\alpha_k} = \frac{1}{k!}\sum_{i=1}^{k!} A_{P_i(\alpha_1\cdots\alpha_k)}, \qquad (31)$$

where P_i denotes the operator of i successive permutations among indices $\alpha_1,\ldots,\alpha_k$. In addition, we assume $\boldsymbol{M}^{[0]} = \mathrm{tr}\boldsymbol{M}^{[2]} = (R^2/4\pi)\int \mathrm{d}\boldsymbol{n}\, g(\boldsymbol{R})$ and $\boldsymbol{M}^{[-2]} = 0$.

The set of equations (30), if we consider it in its entirety, is equivalent to Eq. (28). What we have gained by writing Eq. (28) in the form (30) is the possibility of recognizing slow and fast variables. By limiting ourselves only to the slow ones, we hope to arrive at a simplified (reduced) version of Eq. (28).

We begin by making a few observations about the hierarchy (30). We see that the equation for the kth-order moment involves $(k-2)$th- and $(k+2)$th-order moments. The coupling to the higher order moments appears only in the terms representing the advection [the first three terms on the right-hand side of Eq. (30)]. In the absence of the externally imposed flow (i.e., $\mathrm{Pe}=0$) the hierarchy is thus uncoupled. If we choose any $k=2,4,6,\ldots$, we obtain a closed set of equations. As $t\to\infty$, all the moments approach their equilibrium values. Moreover, we see that the higher is the order of the moment, the faster is the approach. Indeed, the angular part of the second-order differential operator in irreversible part of the Eq. (28) is proportional to the Laplace operator $\mathcal{L} = (\partial/\partial\boldsymbol{n})\cdot(\partial/\partial\boldsymbol{n})$ in the angular variables. This operator has a discrete spectrum with spherical harmonics, which are linear combinations of the moment kernels $w^{[m]}_{\alpha_1\cdots\alpha_m} = n_{\alpha_1}\cdots n_{\alpha_m}$, as its eigenfunctions. In particular, kth harmonics is a linear combination of k functions $w^{[m]}$, with $m\leqslant k$, and its corresponding eigenvalue is $k(k+1)$ which appears in Eq. (30) as a multiplicative factor in the fifth term on its right-hand side. Consequently, there clearly exists a separation of relation times in the space of angular variables of the vector $\boldsymbol{R}$. This consideration implies that $M^{[2]}$ is the slowest (in the absence of external forcing) variable among the moments $\boldsymbol{M}^{[k]}$. We shall therefore suggest to choose it as the state variable in our reduced formulation of Eq. (28). To simplify the notation, we shall use hereafter $M^{[2]} = \boldsymbol{m}$.

Another argument supporting this choice is the observation that the stress tensor (29) turns out to be expressed only in terms of $\boldsymbol{m}$:

$$\boldsymbol{\sigma} = -\left(1+\frac{5}{2}\phi\right)D_{\alpha\beta} - \frac{27}{2}\frac{\phi^2}{\mathrm{Pe}}\Bigg\{2[1-\mu_1(2)]\mathring{\boldsymbol{m}}(2) - \int_2^\infty \mathrm{d}R\left(R\frac{\partial U_{\mathrm{nl}}}{\partial R}(1-\mu_1) + 3(\mu_1-\mu_2) + R\frac{\partial}{\partial R}\mu_1\right)\mathring{\boldsymbol{m}}\Bigg\}, \qquad (32)$$

where $\mathring{\boldsymbol{m}} = \boldsymbol{m} - \frac{1}{3}\boldsymbol{\delta}\,\mathrm{tr}\,\boldsymbol{m}$. As we see from Eq. (32), the extra stress tensor depends indeed only on $\boldsymbol{m}$, and moreover, the dependence on $\boldsymbol{m}$ is linear.

If we now switch on the imposed flow, the first three terms on the right-hand side of Eq. (30) are different from zero and consequently the hierarchy (30) becomes coupled. In particular, we see that the equation governing the time evolution of $\boldsymbol{m}$ involves also the moment $\boldsymbol{M}^{[4]}$. However, as we see in Eq. (30), the terms representing the coupling are all multiplied by the Péclet number. This means that if the Péclet number is small, we can still expect the second moment to evolve in time in a slower pace than the fourth moment, which itself evolves in a slower pace than the sixth moment, etc. Even for larger Péclet numbers, the second moment is still very likely an appropriate state variable. Our numerical predictions of the microstructure and rheology presented below indicate that this is indeed the case. The above three arguments support our hypothesis that the time evolution generated by the Smoluchowski equations and the time evolution generated by an appropriately constructed equation governing the time evolution of $\boldsymbol{m}(R)$ (called hereafter the mS equation) are essentially identical provided we look at the slow part of the time evolution. Below, we shall find the mS equation and in Secs. V A and V B investigate its solutions.

If we put $k=2$ in Eq. (30), we obtain an equation governing the time evolution of $\boldsymbol{m}$:

$$\frac{\partial \boldsymbol{m}}{\partial t} = \mathrm{Pe}\Bigg\{ \boldsymbol{\omega}\cdot\boldsymbol{m} - \boldsymbol{m}\cdot\boldsymbol{\omega} + \frac{\partial}{\partial R}R(\mu_1 - 1)\boldsymbol{M}^{[4]}{:}\boldsymbol{D} + (1-\mu_2) \times(\boldsymbol{D}\cdot\boldsymbol{m} + \boldsymbol{m}\cdot\boldsymbol{D} - 2\boldsymbol{M}^{[4]}{:}\boldsymbol{D})\Bigg\} + \frac{\partial}{\partial R}\sigma_1\hat{g}_{\mathrm{eq}}\frac{\partial}{\partial R}\frac{\boldsymbol{m}}{\hat{g}_{\mathrm{eq}}} - 6\frac{\sigma_2}{R^2}\mathring{\boldsymbol{m}}. \qquad (33)$$

This equation involves so far unspecified fourth order moment $\boldsymbol{M}^{[4]}$. In order to continue, we have to express it in terms of the second order moment $\boldsymbol{m}$. The function $\boldsymbol{W}{:}\boldsymbol{m}\mapsto M^{[4]}$ is called a closure. An ultimate criterion for choosing the closure is the requirement that solutions to the closed equation (i.e., to the mS equation) approximate well solutions to the Smoluchowski equation if we pay most attention to asymptotic ($t\to\infty$) behavior and to the rheological predictions. Such a criterion is obviously difficult to put into practical use. In Appendix B we derive a simple *fourth-order* (in terms of normalized moments) closure by requiring some specific conditions. They are symmetry, normalization, frame indifference, positive definitness, and an exact match in two important limiting cases—namely, in the weak flow (i.e., near equilibrium, $\mathrm{Pe}\ll 1$) and in the strong flows (i.e., when $\mathrm{Pe}\to\infty$ in uniaxial and biaxial elongation flows). With this closure, the expression $\boldsymbol{M}^{[4]}{:}D$ appearing in Eq. (33) becomes

$$\boldsymbol{M}^{[4]}{:}\boldsymbol{D} = \sum_{n=0}^{4}\boldsymbol{M}^{[4]}_{(n)}{:}\boldsymbol{D},$$

$$\boldsymbol{M}^{[4]}_{(0)}{:}\boldsymbol{D} = \frac{2}{15}\boldsymbol{D},$$

$$\boldsymbol{M}^{[4]}_{(1)}{:}\boldsymbol{D} = \frac{2}{15}\mathrm{tr}(\boldsymbol{m}-\boldsymbol{m}_{\mathrm{eq}})\boldsymbol{D} + \frac{1}{7}[\delta\mathring{\boldsymbol{m}}{:}\boldsymbol{D} + 2(\mathring{\boldsymbol{m}}\cdot\boldsymbol{D} + \boldsymbol{D}\cdot\mathring{\boldsymbol{m}})],$$

$$\boldsymbol{M}^{[4]}_{(2)}{:}\boldsymbol{D} = \frac{1}{\mathrm{tr}\,\boldsymbol{m}}\left(\frac{4}{105}I_2\boldsymbol{D} - \frac{2}{21}[\delta(\mathring{\boldsymbol{m}}\cdot\mathring{\boldsymbol{m}}){:}\boldsymbol{D} + 2(\mathring{\boldsymbol{m}}\cdot\mathring{\boldsymbol{m}}\cdot\boldsymbol{D} + \boldsymbol{D}\cdot\mathring{\boldsymbol{m}}\cdot\mathring{\boldsymbol{m}})] + \frac{1}{3}(\mathring{\boldsymbol{m}}\mathring{\boldsymbol{m}}{:}\boldsymbol{D} + 2\mathring{\boldsymbol{m}}\cdot\boldsymbol{D}\cdot\mathring{\boldsymbol{m}})\right),$$

$$\boldsymbol{M}^{[4]}_{(3)}{:}\boldsymbol{D} = \frac{1}{(\mathrm{tr}\,\boldsymbol{m})^2}\left(\frac{8}{45}I_3\boldsymbol{D} + \frac{1}{7}I_2[\delta\mathring{\boldsymbol{m}}{:}\boldsymbol{D} + 2(\mathring{\boldsymbol{m}}\cdot\boldsymbol{D} + \boldsymbol{D}\cdot\mathring{\boldsymbol{m}})] - \frac{1}{3}[\mathring{\boldsymbol{m}}(\mathring{\boldsymbol{m}}\cdot\mathring{\boldsymbol{m}}){:}\boldsymbol{D} + (\mathring{\boldsymbol{m}}\cdot\mathring{\boldsymbol{m}})\mathring{\boldsymbol{m}}{:}\boldsymbol{D} + 2(\mathring{\boldsymbol{m}}\cdot\boldsymbol{D}\cdot\mathring{\boldsymbol{m}}\cdot\mathring{\boldsymbol{m}} + \mathring{\boldsymbol{m}}\cdot\mathring{\boldsymbol{m}}\cdot\boldsymbol{D}\cdot\mathring{\boldsymbol{m}})]\right),$$

$$\boldsymbol{M}^{[4]}_{(4)}{:}\boldsymbol{D} = \frac{1}{(\mathrm{tr}\,\boldsymbol{m})^3}\left(-\frac{4}{21}I_3[\delta\mathring{\boldsymbol{m}}{:}\boldsymbol{D} + 2(\mathring{\boldsymbol{m}}\cdot\boldsymbol{D} + \boldsymbol{D}\cdot\mathring{\boldsymbol{m}})] - \frac{4}{7}I_2[\delta(\mathring{\boldsymbol{m}}\cdot\mathring{\boldsymbol{m}}){:}\boldsymbol{D} + 2(\mathring{\boldsymbol{m}}\cdot\mathring{\boldsymbol{m}}\cdot\boldsymbol{D} + \boldsymbol{D}\cdot\mathring{\boldsymbol{m}}\cdot\mathring{\boldsymbol{m}})] + 2[\mathring{\boldsymbol{m}}\cdot\mathring{\boldsymbol{m}}(\mathring{\boldsymbol{m}}\cdot\mathring{\boldsymbol{m}}){:}\boldsymbol{D} + 2\mathring{\boldsymbol{m}}\cdot\mathring{\boldsymbol{m}}\cdot\boldsymbol{D}\cdot\mathring{\boldsymbol{m}}\cdot\mathring{\boldsymbol{m}}]\right), \qquad (34)$$

where I_2 and I_3 are the second and third invariants of the tensor $\mathring{\boldsymbol{m}}$:

$$I_2 = \mathrm{tr}(\mathring{\boldsymbol{m}}\cdot\mathring{\boldsymbol{m}}), \quad I_3 = \mathrm{tr}(\mathring{\boldsymbol{m}}\cdot\mathring{\boldsymbol{m}}\cdot\mathring{\boldsymbol{m}}).$$

To complete the formulation of the mS equation, we have to supply the boundary conditions. We derive them from Eqs. (6) and (9) by making appropriate averages:

$$(\boldsymbol{m}/R^2)|_{R\to\infty} \to \frac{1}{3}g_{\mathrm{eq}}\delta,$$

$$\left[\sigma_1 g_{\mathrm{eq}}R\frac{\partial}{\partial R}\frac{\boldsymbol{m}}{\hat{g}_{\mathrm{eq}}}\right]\Bigg|_{R=2} + \mathrm{Pe}[\mu_1(2)-1]\boldsymbol{M}^{[4]}|_{\boldsymbol{m}=\boldsymbol{m}(2)}{:}\boldsymbol{D} = 0. \qquad (35)$$

Summing up, we have identified a reduced Smoluchowski equation, called the mS equation, whose solutions have the following properties: (i) If $\mathrm{Pe}=0$, then the asymptotic (i.e., equilibrium) solutions of the Smoluchowski equation and of the mS equation are identical (in the sense that the second moment of the equilibrium solution of the Smoluchowski equation equals the equilibrium solution of the mS equation). Both the Smoluchowski and mS equations are compatible with thermodynamics. (ii) If the Péclet number is small, then, for large times, solutions to the mS equation approximate well solutions to the Smoluchowski equation.

In order to situate our approach to finding solutions to the Smoluchowski equation, we compare it with the approaches to the same problem developed in [3,7,6]. The starting point in all three papers is an ansatz about the form of the solution.

Phan-Thien [3] assumes that the solutions have a δ-function-like behavior in the dependence on R [i.e., the solution is proportional to $\delta(R-\hat{R})$]. In concentrated suspensions this may indeed be a good approximation with $\hat{R}$ being the surface of the particle. In this paper we do not consider concentrated suspensions. The dependence on R does not show a sharp peak about any value of R.

Hess [7] does not discuss rheology and does not include hydrodynamic interactions. The ansatz used by Hess is the following: $g(\boldsymbol{R})-g_{\mathrm{eq}}(\boldsymbol{R})\sim a_{\alpha\beta}R_\alpha R_\beta h(R)$, where g_{eq} is the correlation function at equilibrium and $a_{\alpha\beta} = \int d\boldsymbol{R}g(\boldsymbol{R})R_\alpha R_\beta h(R)$, where $h(R)$ is a cut off function (i.e., a function that approaches zero sufficiently rapidly as $R\to\infty$ so that the integral exists). Hess uses thus the assumption of the separation of scales. As appears from our analysis, such a separation indeed exists but only in the angular dependence of $g(\boldsymbol{R})$. We do not make any assumption of this type in the radial dependence. The disadvantage of our approach is that we do not calculate the pair correlation function $g(\boldsymbol{R})$ [we calculate only its moments $\boldsymbol{m}(R)$] and thus the structure factor [the Fourier transform of $g(\boldsymbol{R})$, a quantity that is observed in optical measurements] is missing in the list of our results.

The authors of [6] do not include hydrodynamic interactions and consider only the hard-core interparticle potential. Their ansatz is that $g(\boldsymbol{R})$ is expanded in a finite number of functions introduced by [29]. In Sec. V B we shall compare our results (for the particular case when the hydrodynamic interactions are absent) with the results obtained in [6].

V. PREDICTIONS OF MICROSTRUCTURE AND RHEOLOGICAL PROPERTIES

In order to arrive at data collected in rheological observations, we have to first solve the set of partial differential equations (33) for six independent components of the tensor $\boldsymbol{m}(R,t)$. The complexity of this task is considerably reduced relative to the complexity of the task of solving numerically the original Smoluchowski equation (28). Due to the unbounded domain of the variable R and the nonpolynomial nonlinearity appearing in the closure relations, the problem of solving numerically Eq. (33) remains still, however, a nonroutine problem. We solve the unboundedness of the domain by changing the variables $[R \to x(R)=1/R]$ and the nonpolynomial nonlinearity by using a nonlinear version of the Galerkin method known as the *group finite-element method* [30]. Details of the numerical approach are given in Appendix C.

In the context of the mS equations (33) and (32), the microstructure of the suspension is characterized by the microstructure tensor

$$\boldsymbol{m}^*(R) = \frac{1}{R^2}\boldsymbol{m} = \frac{1}{4\pi}\int \mathrm{d}\boldsymbol{n}\boldsymbol{n}\boldsymbol{n}g(\boldsymbol{R}).$$

As follows from its definition, the absence of pair correlations (i.e., the absence of microstructure in HI suspensions) means that the microstructure tensor is proportional to the unit tensor: namely, $\boldsymbol{m}^*(\boldsymbol{R})=(1/3)\boldsymbol{\delta}$. The nonzero tensor $\boldsymbol{q} = \boldsymbol{m}^*(\boldsymbol{R}) - \frac{1}{3}\boldsymbol{\delta}$ indicates the presence of the microstructure which can be induced either by direct interparticle interactions (hard-core or nonlocal particle-particle interactions) or by flow through advection and hydrodynamic interactions. In the absence of flow, direct interaction forces create equilibrium correlations $\boldsymbol{m}^*_{\mathrm{eq}}(R)=(1/3)g_{\mathrm{eq}}(R)\boldsymbol{\delta}$ which are isotropic and depend only on the interparticle distance R. The anisotropy generated by the imposed overall flow creates an anisotropy in the microstructure, so that the tensor $\boldsymbol{m}^*$ is no longer proportional to $\boldsymbol{\delta}$. Such an anisotropy is created, on the one hand, by the combined influence of the advection and direct interactions and, on the other hand, by hydrodynamic interactions that are anisotropic by their nature.

In order to expose the effect of hydrodynamic interactions on the microstructure and rheology, we shall investigate suspensions both with and without hydrodynamic interactions. In the absence of hydrodynamic interactions (i.e., if we put $\boldsymbol{\lambda}=0$ and $\boldsymbol{\Lambda}=\boldsymbol{\delta}$), the suspensions will be called direct-interaction (DI) suspensions. The singular behavior of the hard-core potential does not enter explicitly their governing equations since we take into account the potential U_{HC} in the boundary condition (9). Two types of DI suspensions will be investigated: one with only the hard-core potential and the other with the hard-core potential together with the nonlocal potential (5).

In both HI and DI suspensions we consider only two-particle interactions. Since the contributions of k-particle interactions to the stress are proportional to ϕ^k, where ϕ is the volume fraction of the suspended particles, we shall present the stresses in the form $\boldsymbol{\sigma}/\phi^2$.

Below, we present microstructural and rheological responses to viscometric flows (i.e., homogeneous shear and elongation flows that are, as for their dependence on time, either start up or oscillatory). Linear responses to oscillatory flows implied by the Smoluchowski equation are well known [12,13]. The results presented in Sec. V A serve thus (i) to complete the list of the rheological predictions, (ii) to confirm, in this particular case, that the consequences of the mS model and the Smoluchowski equation are identical, and (iii) to compare the linear responses with the nonlinear responses presented in the subsequent subsection. Nonlinear responses to shear and elongation flows, presented in Sec. V B, have not been, to the best of our knowledge, calculated before.

A. Linear response solution

In this section we look at small linear perturbations of equilibrium caused by weak oscillatory shear flows with the rate of strain $\boldsymbol{D}=\boldsymbol{D}_0 e^{i\omega t}$. The linear response solution to Eq. (33) has a general form

$$\boldsymbol{m} = \hat{g}_{\mathrm{eq}}\left(\frac{1}{3}\delta + \mathrm{Pe}\, f\boldsymbol{D}_0 e^{i\omega t}\right), \tag{36}$$

where $f(R)$, called a linear response function, is at this point an unknown function. In terms of the correlation function the ansatz (36) looks like

$$g = g_{\mathrm{eq}}\left(1 + \frac{15}{2}\mathrm{Pe}\, f\boldsymbol{n}\boldsymbol{n}\!:\!\boldsymbol{D}_0 e^{i\omega t}\right). \tag{37}$$

It is important to realize that both the Smoluchowski equation (28) and the mS equation (33) are completely equivalent from the point of view of linear response theory (i.e., they lead to the same linear perturbation solution). This is because the closure relation for the fourth moment has been chosen to be consistent with the equilibrium solution.

Substituting the expressions (36) into Eq. (33) and keeping only linear terms with respect to $\boldsymbol{D}$, we obtain the following equation determining the linear response function f:

$$\frac{\partial}{\partial R}\sigma_1\hat{g}_{\mathrm{eq}}\frac{\partial}{\partial R}f - f\hat{g}_{\mathrm{eq}}\left(\frac{6\sigma_2}{R^2} + i\omega\right) = -\frac{2}{15}\hat{g}_{\mathrm{eq}}\left(R\frac{\partial U_{\mathrm{nl}}}{\partial R}(1-\mu_1) + R\frac{\partial \mu_1}{\partial R} + 3(\mu_1 - \mu_2)\right). \tag{38}$$

We impose the following boundary conditions:

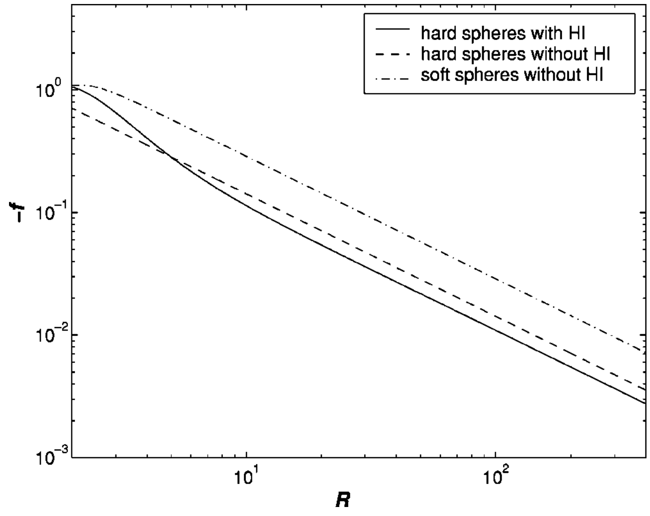

FIG. 1. Dependence of the linear response function f (dimensionless) on interparticle distance R (presented in dimensionless units R/a) in a stationary flow ($\omega=0$) of suspensions of hard spheres with and without HI and suspension of soft spheres without HI interacting by nonlocal potential U_{nl}, Eq. (5), with $\epsilon=10^4$.

$$f|_{R\to\infty} \to 0,$$

$$\sigma_1 \frac{\partial f}{\partial R}\bigg|_{R\to 2} + \frac{4}{15}[\mu_1(2)-1] = 0, \qquad (39)$$

derived from the conditions (6) and (9) by omitting all nonlinear terms in $\boldsymbol{D}$.

We solve Eq. (38) by applying a numerical method that is a linearized version of the method that we use below for the nonlinear problem [see Eq. (C4) in Appendix C].

Let us look first at stationary flows ($\omega=0$). The remarkable fact that we note is that the function $f_0=f|(\omega=0)$ is a nonpositive function (see Fig. 1) both in the presence and absence of hydrodynamic interactions. The nonpositivity of f_0 is a consequence of the nonpositivity of the right-hand side of Eq. (38). The consequences of the negative sign of the response function f_0 can be easily seen in Eq. (36). Let $\boldsymbol{D}_0$ be diagonal (this can be achieved by choosing appropriately the coordinate system). We see from Eq. (36) that $\boldsymbol{m}$ is also diagonal. Moreover, we see that the larger is the entry of $\boldsymbol{D}_0$ (note that larger entry means larger stretching of the imposed flow), the smaller is the corresponding entry of the microstructural tensor $\boldsymbol{m}$. This means that the correlations are larger in the direction of the contraction of the imposed flow and not in the direction of its stretching as it is in the case of polymeric suspensions. This effect persists in the nonlinear response. We shall see it in the next subsection.

By inserting Eq. (36) into the expression (29), we find the effective complex viscosity

$$\eta^*(\omega) = \eta_0\left(1 + \frac{5}{2}\varphi + K(\omega)\varphi^2\right), \qquad (40)$$

where the function $K(\omega)$ is defined as

$$K(\omega) = \frac{27}{2}\Bigg\{8g_{\mathrm{eq}}(2)[\mu_1(2)-1]f(2,\omega) + \int_2^\infty \mathrm{d}R g_{\mathrm{eq}} R^2 f(R,\omega) \times\left[R\frac{\partial\mu_1}{\partial R} + R\frac{\partial U_{\mathrm{nl}}}{\partial R}(1-\mu_1) + 3(\mu_1-\mu_2)\right]\Bigg\}. \qquad (41)$$

Beside the complex viscosity, the quantity of interest in oscillatory flows is the complex modulus $G^*=G'+iG''$ related to the complex viscosity $\eta^*(\omega)$ as follows: $G^*=i\omega\eta^*$.

Figure 2 shows elastic modulus G' and effective viscosity η' as functions of the frequency ω.

We observe that $G'(\omega)$ reaches a constant value (G'_∞) in the limit $\omega\to\infty$. Here we have to pose and note that at sufficiently high frequencies we eventually reach the time scales $t\ll\tau_{\mathrm{S}}$, which are out of the realm of the applicability of the Smoluchowski equation (1) and, in fact, also the Fokker-Planck equation. We observe, however, that the quantity $G'(\omega)$ reaches the limit G'_∞ at frequencies that still remain within the domain of applicability at least in the case of HI suspensions. Indeed, the plateau for $G'(\omega)$ starts at $\omega\approx 10$ for HI suspensions and at $\omega\approx 10^6$ for DI suspensions. We should stress again that the high-frequency limits for the mS equation and Smoluchowski equation are completely identical because of the equivalence of these two equations in linear near-equilibrium approximation. The well-known (see, for example, [12,13]) analytical estimation for the value G'_∞ in HI suspensions is

$$G'_\infty \approx \frac{9}{5}\varphi^2\int_2^\infty \mathrm{d}R R^2 g_{\mathrm{eq}}\left[R\frac{\partial U_{\mathrm{nl}}}{\partial R}(1-\mu_1) + R\frac{\partial\mu_1}{\partial R} + 3(\mu_1-\mu_2)\right]^2. \qquad (42)$$

For hard spheres with hydrodynamic interactions this quantity takes the value

$$G'_\infty \approx 35.56,$$

and it coincides well with the limit reached in our computations. We are unable to derive a similar analytical estimate for G'_∞ in the case of DI suspensions.

B. Nonlinear response to start up and steady shear and elongation flows

We denote the normalized dimensionless gradient of velocity by $L_{\alpha\beta}=\dot{\gamma}^{-1}\partial v_\alpha/\partial r_\beta$, where $\dot{\gamma}=(\partial v_\alpha/\partial r_\beta)(\partial v_\beta/\partial r_\alpha)^{1/2}$. In the simple shear flow,

$$\boldsymbol{L} = \begin{bmatrix} 0 & 1 & 0 \\ 0 & 0 & 0 \\ 0 & 0 & 0 \end{bmatrix}, \qquad (43)$$

and in the elongation flow,

$$\boldsymbol{L} = \frac{1}{\sqrt{6}}\begin{bmatrix} 2 & 0 & 0 \\ 0 & -1 & 0 \\ 0 & 0 & -1 \end{bmatrix}. \qquad (44)$$

First, we analyze how the microstructure changes in start up flows. In our numerical calculations, the suspension rests ini-

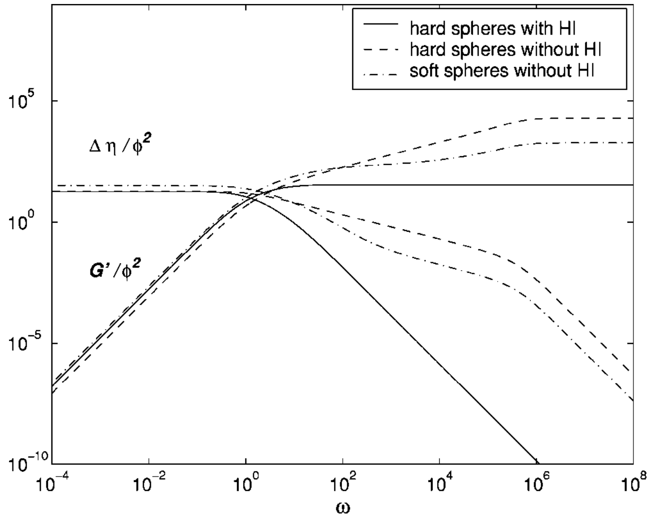

FIG. 2. The dimensionless effective viscosity $\Delta\eta=[\mathrm{Re}(\eta^*)-\eta_{\rm hydr}]/\eta_0$, where $\eta_{\rm hydr}=\eta_0[1+(5/2)\phi]$, and the dimensionless elastic modulus $G'=\mathrm{Re}(G^*)/G_0$, where $G_0=\eta_0/\tau_{\rm S}$ and $\tau_{\rm S}$ is given by Eq. (26), as functions of dimensionless frequency ω (as transformed from dimensional form $\omega\to\omega\tau_{\rm S}$) for suspensions of hard spheres with and without HI and suspensions of soft spheres without HI. Soft spheres interact directly by nonlocal potential, Eq. (5) with $\epsilon=10^4$, in addition to the hard-core potential, Eq. (4).

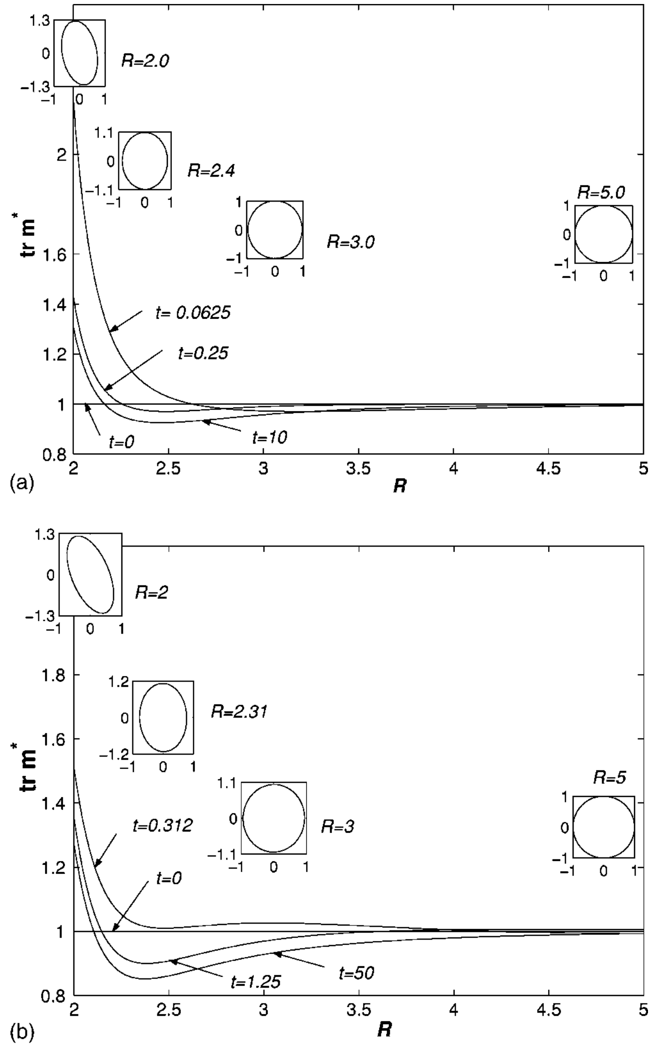

FIG. 3. Trace of the dimensionless microstructure tensor, tr $\boldsymbol{m}^*$, and the correlation ellipses in a moderately strong shear flow (Pe $=10$) of suspension of hard spheres (a) with HI and (b) without HI. All correlation ellipses correspond to $t=10$ for figure (a) and $t=50$ for figure (b). Time t and distance R are presented in dimensionless units $t\to t/\tau_{\rm S}$, where $\tau_{\rm S}$ is given by Eq. (26), and $R\to R/a$.

tially at equilibrium ($g=g_{\rm eq},\boldsymbol{L}=0$); then, at time $t=0$, the overall velocity gradient Pe$\boldsymbol{L}$ jumps instantly from zero to its steady value. Figures 3 and 4 show the behavior of the microstructure tensor $\boldsymbol{m}^*$ for two cases: suspension of hard spheres with and without hydrodynamic interactions. We represent the tensor $\boldsymbol{m}^*$ by its trace and correlation ellipses defined as projections of ellipsoids described by the equation

$$\sum_{ij=1}^{3} x_i(\boldsymbol{m}^*)^{-1}_{ij}x_j=\frac{3}{g_{\rm eq}\mathrm{tr}\,\boldsymbol{m}^*} \tag{45}$$

on the (x_1,x_2) plane. The normalization factor tr $\boldsymbol{m}^* g_{\rm eq}(R)/3$ is chosen in such a way that the correlation ellipse (45) at the equilibrium state is represented by a sphere with unit radius (for any R). In both flows, Eqs. (43) and (44), the third coordinate is not important due to the translational symmetry along the x_3 axis in shear flow and the rotational symmetry in the (x_2,x_3) plane in the elongational flow. Consequently, projection on the plane $x_3=0$ provides enough information about the microstructure.

We observe that at large R, in all suspensions, the correlation ellipses become circles. This indicates that the correlation anisotropy decays when R increases. For small R, the anisotropy of the microstructure is significant. We observe that in both suspensions the direction of the major axis of the correlation ellipse is inclined towards the direction of the strongest flow compression (i.e., towards the direction of the eigenvectors corresponding to smallest eigenvalue of the rate of strain tensor $\boldsymbol{D}$) and not towards the flow stretching like in the case of polymeric solutions. In the latter case the microstructure tensor characterizes the orientation of polymeric molecules in the physical space (more precisely, orientation of molecules coincides with the orientation of the ellipsoid of correlations induced by intramolecular forces). This effect can be seen as a nonlinear version of the nonpositivity of the linear response that was observed in the linear case (see the preceding subsection). The difference that we have just noted is explained by the difference in the character of the interactions. The forces generated by the hard-core potential as well as the forces generated by hydrodynamic interaction have a repelling character. The interaction forces decrease with increasing the distance while the intramolecule forces in polymeric solutions are attractive and increase with increasing the distance.

Next, we discuss standard viscometric quantities associated with the start up shear and elongation flows. Here we have to repeat the comment that we have made in the previous subsection in the context of the limit $\omega\to\infty$. Indeed, reactions to start-up flows are determined, in the initial small period, by fast processes that are outside of our model. The

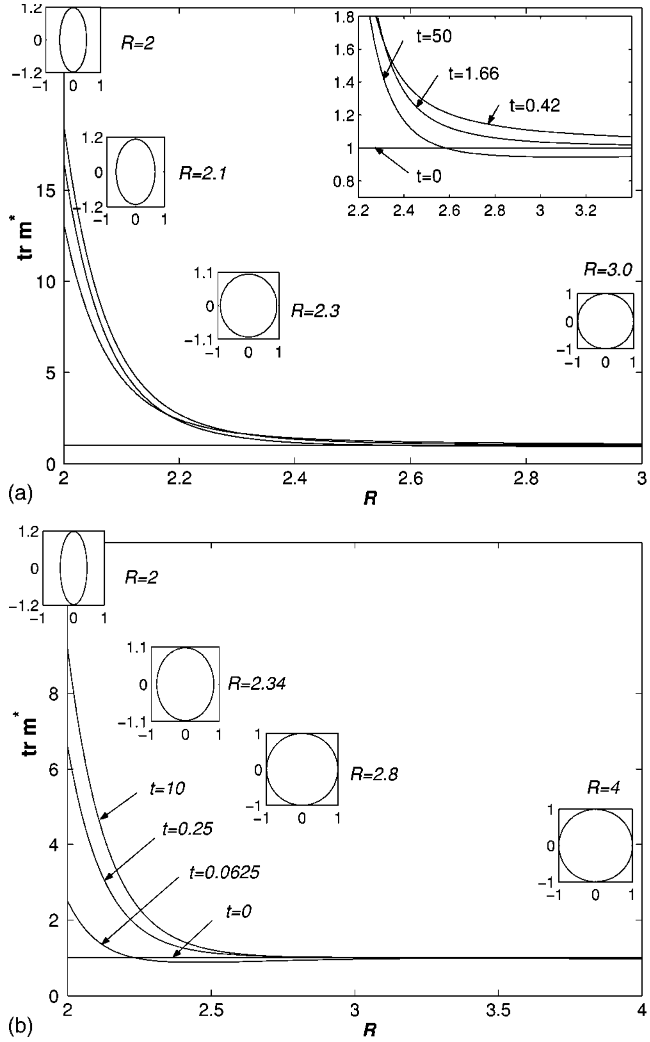

FIG. 4. Trace of the microstructure tensor, tr $\boldsymbol{m}^*$, and correlation ellipses in moderately strong elongation flow (Pe=10) of suspensions of hard spheres (a) with HI and (b) without HI. All correlation ellipses correspond to $t=50$ for figure (a) and $t=10$ for figure (b). Time t and distance R are presented in dimensionless units $t \rightarrow t/\tau_S$, where τ_S is given by Eq. (26), and $R \rightarrow R/a$.

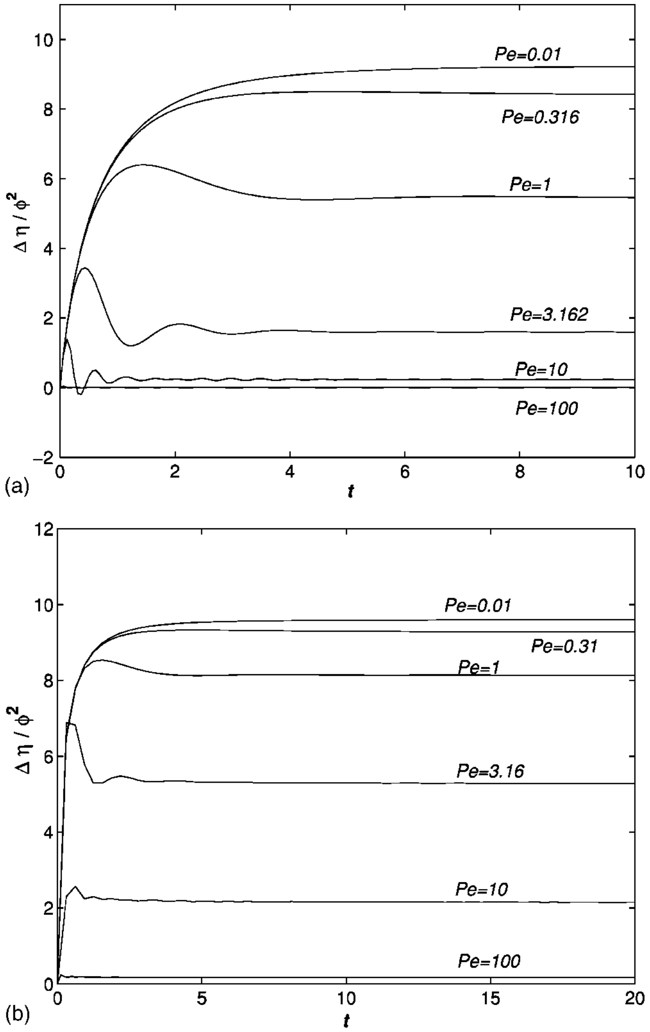

FIG. 5. Time dependence of the dimensionless and normalized particle shear viscosity, $\Delta\eta = \eta_s - \eta_{\mathrm{hydr}}$, where $\eta_{\mathrm{hydr}} = 1 + 5\phi/2$ and η_s is defined in Eq. (46) in start-up simple shear flow of suspensions of hard spheres (a) with HI (b) without HI. Time t is presented in dimensionless units $t \rightarrow t/\tau_S$, where τ_S is given by Eq. (26).

natural averaging made by experimental apparatus recording the reaction of the suspension may however bring the observed behavior to the realm of our model. A detailed discussion of this point is clearly beyond the scope of this paper. In the case of the start up shear flow, these quantities are (in terms of the dimensional variables) the normalized shear viscosity $\eta_s = -\sigma_{12}/\dot{\gamma}$, the normalized first and the second normal stress coefficients $\psi_1 = (\sigma_{22} - \sigma_{11})/\dot{\gamma}^2$, $\psi_2 = (\sigma_{33} - \sigma_{22})/\dot{\gamma}^2$, where $\sigma_{\alpha\beta}$ are the components of the dimensional extra stress tensor. In the elongation flow, the only interesting viscometric parameter is the normalized elongation viscosity $\eta_{\mathrm{el}} = (\sigma_{22} - \sigma_{11})/\dot{\gamma}$. After the transformation to dimensionless variables (see the Sec. III B) these quantities become

$$\eta_s = -\sigma_{12}, \tag{46}$$

$$\psi_1 = \mathrm{Pe}^{-1}(\sigma_{22} - \sigma_{11}), \tag{47}$$

$$\psi_2 = \mathrm{Pe}^{-1}(\sigma_{33} - \sigma_{22}), \tag{48}$$

$$\eta_{\mathrm{el}} = \sigma_{22} - \sigma_{11}, \tag{49}$$

where $\boldsymbol{\sigma}$ is a dimensionless stress tensor.

Figures 5–9 show rheological predictions for HI suspension as well as DI suspensions. We are comparing them in order to observe similarities and differences in the effects produced by hydrodynamic interactions in combination with hard-core interparticle interactions and by purely hard-core interactions.

In the shear flow our predictions confirm experimentally observed [4] shear and normal stress thinning behavior (i.e., decay with growth of Pe number) in HI suspensions at least for Pe ranging from 0 to 500. The same behavior pertains in DI suspensions. In the time evolution of all rheological quantities we observe an "overshot" followed, in some cases, by weak and strongly damped oscillations before reaching steady-state values. The overshoots and the damped oscilla-

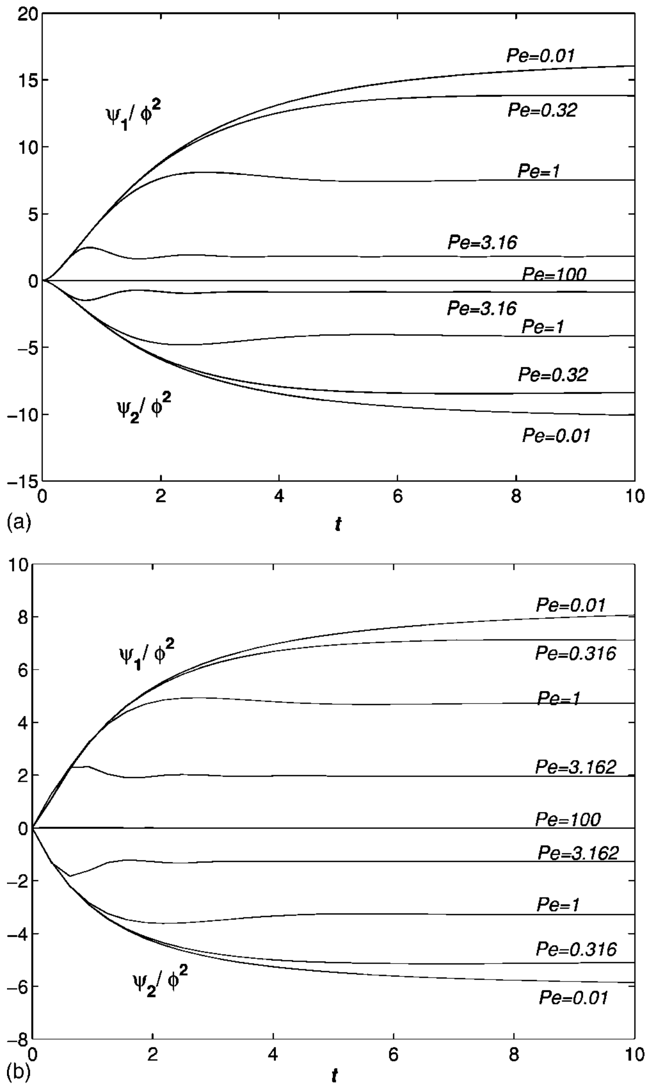

FIG. 6. Time dependence of the dimensionless normalized first (47) and second (48) normal stress coefficients in start-up simple shear flow of suspensions of hard spheres (a) with HI and (b) without HI. Time t is presented in dimensionless units $t \to t/\tau_S$, where τ_S is given by Eq. (26).

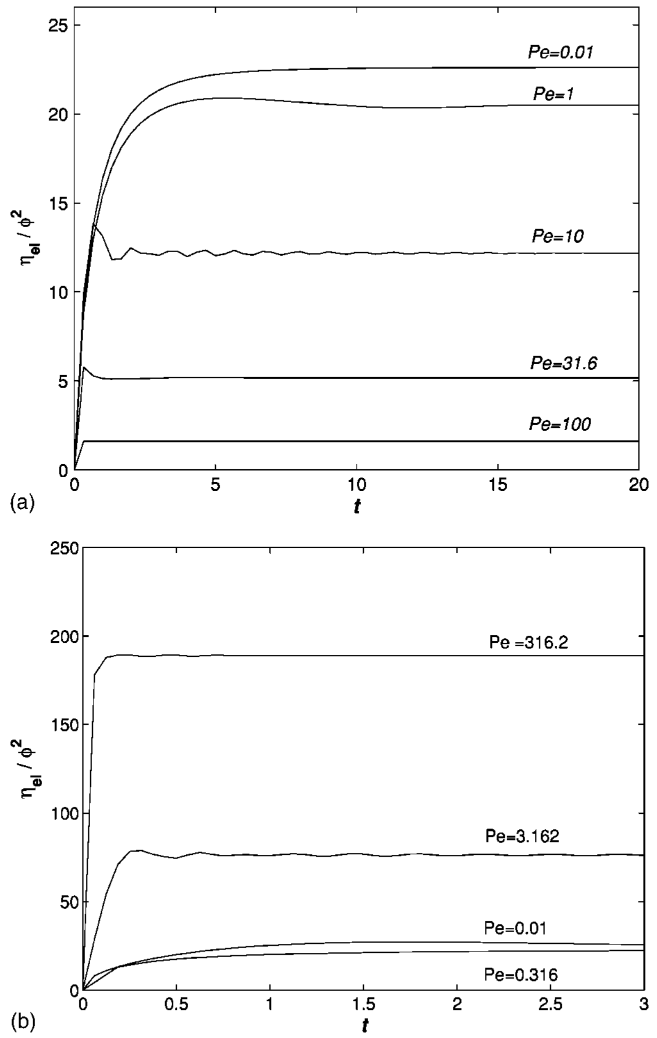

FIG. 7. Time dependence of the dimensionless normalized elongation viscosity (49) in start-up elongation flow of suspensions of hard spheres (a) with HI and (b) without HI. Time t is presented in dimensionless units $t \to t/\tau_S$, where τ_S is given by Eq. (26).

tions are more pronounced in flows with moderate Péclet number, Pe, and are negligible for small and large Pe.

Another observation concerns the second normal stress coefficient which in our tests appears to be, at steady states, negative, in both HI and DI suspensions. This is in accordance with observations made by other researchers [4], but in disagreement with Phan-Thien [3].

We also note that within the tested range of Péclet numbers we do not see the thickening behavior (i.e., increase with increasing Pe). Such behavior has been observed in experimental measurements [4] as well as in numerical simulations [5]) in concentrated suspensions and for large Péclet numbers. The reasons why we do not see it may be the following: the thickening effect arises due to the physics that we did not put into our governing equations (e.g., the role of more-than-two particle interactions that certainly play an important role in concentrated suspensions), and/or the thickening effect begin to appear for large Pćlet numbers (larger than $\mathrm{Pe} > 10^2$) for which, due to the stiffness of our discrete equations, we are unable to produce numerical results with sufficient accuracy.

In order to test our method of solution of the Smoluchowski equations we compare our results with results obtained by using other methods. In particular, we compare the predictions for the shear viscosity and the first normal stress coefficient in the case of hard spheres without hydrodynamic interactions with the predictions based on approximate solutions found by Bławzdziewicz and Szamel [6]. We see that our results for the shear viscosity coefficient agree well with the results reported in [6] for small Pe. The first normal stress coefficient as well as the shear viscosity coefficient for large Pe appear to be different. A detail comparison of our and the Bławzdziewicz-Szamel approximations is needed to explain the discrepancy.

Our results for start-up elongation flows reveal a remarkable qualitative difference between HI and DI suspensions. In HI suspensions we see a thinning behavior for the elongation viscosity η_{el} at large Pe while in DI suspension we see

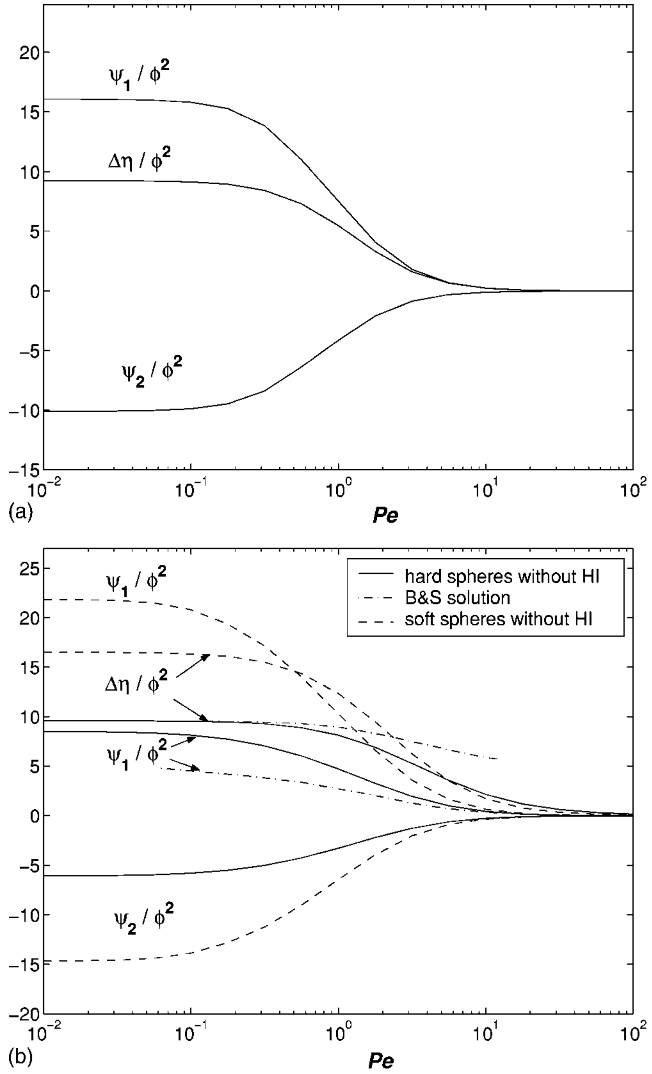

FIG. 8. Steady-state values of the dimensionless normalized particle shear viscosity, $\Delta\eta=\eta_s-\eta_{hydr}$, where $\eta_{hydr}=1+5\phi/2$ and η_{shear} is given in Eq. (46), the dimensionless first (ψ_1) and the second (ψ_2) normal stress coefficients, Eqs. (47) and (47), vs Péclet number Pe in a simple shear flow of suspension of (a) hard spheres with HI and (b) hard and soft spheres without HI. Dash-dotted lines correspond to the approximate solution by Bławzdziewicz and Szamel [6]. Soft spheres interact directly by nonlocal potential, Eq. (5) with $\epsilon=10^4$, in addition to the hard-core potential, Eq. (4).

a thickening behavior. However, we note that at small Pe $(\mathrm{Pe}\ll 1)$, DI suspensions also show a weak thinning behavior.

The difference between the elongation viscosity of HI and DI suspensions is explained by the peculiar behavior of hydrodynamic interactions when two particle are close to each other (R is close to 2). According to the lubrification approximation (see [10,28]), which is used to derive the near-field asymptotic behavior of the function $\sigma_{1,2}$ in Eq. (2) and $\mu_{1,2}$ in Eq. (3), the hydrodynamic interaction compensates the hard-core interaction so that the projection on the normal to the particle surface of the sum of the two forces (one coming from the fluid and the other from the hard core) equals zero at the surface. Consequently, the suspensions with hydrodynamic interaction show much weaker resistance to the flow compression than suspensions with only hard-core interactions. In strong flows, the hard-core interactions create very high strains along directions of the compression because the particles strongly resist being drawn near to each other. However, the strong repulsion is, at least partly, shielded by hydrodynamic interactions, even if the hydrodynamic interactions retain still the repelling character.

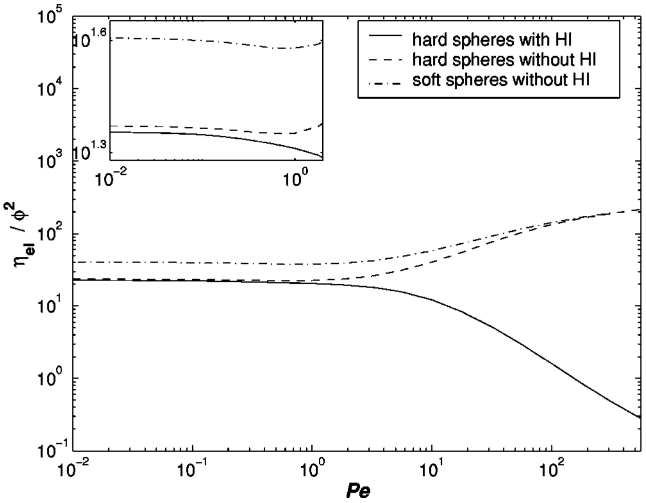

FIG. 9. Steady-state values of the dimensionless elongation viscosity, η_{el}, Eq. (49), vs Peclét number Pe in an elongation flow for suspension of hard spheres with and without HI.

VI. CONCLUDING REMARKS

We have investigated in this paper two types of suspensions: HI and DI suspensions. We shall now compare them with dilute polymeric suspensions that have been extensively studied in the literature (see, e.g., [14]). Before making the comparison we note that the three suspensions are idealizations representing three extreme cases. In real suspensions the features of the above three idealizations are mixed. A better understanding of the relationship between microstructure and rheology in HI, DI, and polymeric suspensions is only a step towards understanding the rheology of real suspensions.

We begin the comparison with the physical settings. All three suspensions are assumed to be isothermal, incompressible, and spatially homogeneous. The fluid in which particles, are suspended is in all three suspensions the same. It is a Newtonian fluid. The suspended particles are structureless (rigid spheres) in HI and DI suspensions and with an internal structure (for example, the particles are modelled as dumbbells) in polymeric suspensions. In all three cases the suspended particles are subjected to the Brownian force and the drag force imposed by flow. In HI suspensions in addition to the latter the suspended particles are subjected to the hydrodynamic interaction. There are no intraparticle forces involved in HI and DI suspensions; there is such force (the force originating from the spring connecting the two spheres of the dumbbell) in polymeric suspensions. Typically, the intraparticle potential in polymeric suspensions is chosen to be proportional to R^2 for small R and reaching infinity for a finite R [the so-called finitely extensible nonlinear elastic (FENE) potential]. There are no interparticle forces involved in the dilute polymeric suspensions; the interparticle force involved in HI and DI suspensions is generated by the hard-core potential (4).

Next, we compare the theoretical descriptions. In all three suspensions the internal structure is chosen to be described by a pair correlation function $g(\boldsymbol{R})$ or alternatively by the microstructure tensor $\boldsymbol{m}^*(R)$, which is the second moment $[\boldsymbol{m}^*(R)=(4\pi)^{-1}\int d\boldsymbol{n}\boldsymbol{n}\boldsymbol{n}g(\boldsymbol{R})$, where $R=|\boldsymbol{R}|$ and $\boldsymbol{n}=\boldsymbol{R}/R]$ of $g(\boldsymbol{R})$ in the unit vector $\boldsymbol{n}$. In polymeric suspensions the vector $\boldsymbol{R}$ is the intraparticle coordinate (the end-to-end vector of the dumbbell that models the particle) and in HI and DI suspensions the vector connecting two suspended particles. The function $g(\boldsymbol{R})$ represents the intraparticle correlation in polymeric suspensions and the pair correlation function of all suspended particles in HI and DI suspensions. The microstructure tensor $\boldsymbol{m}^*(R)$ can be integrated over R only in polymeric suspensions [the tensor $\boldsymbol{m}_c=\int dRR^2\boldsymbol{m}^*(R)$, called a conformation tensor, is a very frequently used microstructural state variable]. In all three suspensions, the equation governing the time evolution of $g(\boldsymbol{R})$ is the Smoluchowski-type equation.

Finally, we compare the microstructure and the rheological behavior. As for the microstructure, there is an essential difference in the responses to flow deformations in polymeric suspensions and suspensions of structureless particles. The "direction of ordering" defined to be the eigenvector of $\boldsymbol{m}(R)$ corresponding to its largest eigenvalue takes the direction of the extension of the imposed flow in polymeric suspensions and the direction of the contraction in suspensions. We have seen it in both the linear and nonlinear responses. The difference is a consequence of the repulsive character of the hydrodynamic and direct hard-core interactions.

Now, we turn to the rheological responses. Although the responses to simple shear flows are qualitatively similar in both polymeric suspension and suspension of structureless particles, we see an essential difference in elongation flows. In shear flows, for all three suspensions, we see shear thinning for the viscosity and the first and second normal stress differences and negative second normal stress coefficient. In elongation flows, the polymeric suspensions (with the FENE potential) always show thickening before reaching a plateau. In HI suspensions we observe thinning and in DI suspensions thickening in the elongation flow. The main reason for all the differences in the rheological behavior of polymeric and structureless particle suspensions is the difference in the character of the forces involved. The intraparticle forces in polymeric molecules are attractive and tend to infinity at larger distances. On the other hand, the interparticle forces as well as the forces generated by hydrodynamic interactions between structureless suspended particles are repulsive and decrease as the interparticle distance increases.

ACKNOWLEDGMENT

This work has been partially supported by the Natural Sciences and Engineering Research Council of Canada.

APPENDIX A: KINETIC COEFFICIENTS $\boldsymbol{\sigma_1,\sigma_2,\mu_1,\mu_2}$

The kinetic coefficients $\boldsymbol{\Lambda}$ and $\boldsymbol{\lambda}$ [see Eqs. (2) and (3)] arise from the microhydrodynamics investigation (Stokes' problem) of the motion of rigid spheres in a Newtonian fluid. It is not our intention in this paper to contribute to the solution of this difficult problem. We shall be content with the approximative solution [28] obtained for two suspended particles. We will work with dimensional notation that were used in Sec. II. In the far-field limit—i.e., in the limit $R\rightarrow\infty$—we use the following approximation [17,28]:

$$\sigma_1 = 1 - \frac{3}{2}\frac{a}{R} + \frac{a^3}{R^3} - \frac{15}{4}\frac{a^4}{R^4} + o((a/R)^6), \tag{A1}$$

$$\sigma_2 = 1 - \frac{3}{4}\frac{a}{R} - \frac{1}{2}\frac{a^3}{R^3} + o((a/R)^6) \tag{A2}$$

and

$$\mu_1 = 5\frac{a^3}{R^3} - 8\frac{a^5}{R^5} + 25\frac{a^6}{R^6} + o((a/R)^7), \tag{A3}$$

$$\mu_2 = \frac{16}{3}\frac{a^5}{R^5} + o((a/R)^6). \tag{A4}$$

In the limit $R\rightarrow 2a$ (the near-field limit) [28],

$$\sigma_1 \rightarrow 2(R/a-2), \tag{A5}$$

$$\sigma_2 \rightarrow 0.401 \tag{A6}$$

and

$$\mu_1 \rightarrow 1 - 4.077(R/a-2), \tag{A7}$$

$$\mu_2 = 0.406. \tag{A8}$$

Here we are keeping only the lower-order polynomial part of Batchelor's solution, dropping higher-order logarithmic functions.

We interpolate both asymptotics by using a simple Padé approximation. Namely, we add higher-order terms with respect to R^{-1} in the far-field approximation and choose coefficients so that the resulting polynomial matches the near-field asymptotics. This procedure results in the following interpolations:

$$\sigma_1 \approx 1 - \frac{3}{2}\frac{a}{R} + \frac{a^3}{R^3} - \frac{15}{4}\frac{a^4}{R^4} + 109.0\frac{a^6}{R^6} - 236.0\frac{a^7}{R^7},$$

$$\sigma_2 \approx 1 - \frac{3}{4}\frac{a}{R} - \frac{1}{2}\frac{a^3}{R^3} - 10.336\frac{a^6}{R^6} \tag{A9}$$

and

$$\mu_1 \approx 5\frac{a^3}{R^3} - 8\frac{a^5}{R^5} + 25\frac{a^6}{R^6} - 423.712\frac{a^7}{R^7} + 907.424\frac{a^8}{R^8},$$

$$\mu_2 \approx \frac{16}{3}\frac{a^5}{R^5} + 15.317\frac{a^6}{R^6}. \tag{A10}$$

We note that the version of the Padé interpolation (A9) has one important property: the functions σ_1 and σ_2 remain nonpositive on entire domain $I=[0,1/2]$. This condition is sufficient to ensure the non-negativity of the matrix $\boldsymbol{\Lambda}$ [see Eq. (2)].

Although there are more accurate and technically more involved solutions [10,21–23,31] to the Stoke's problem that can be used to calculate $\boldsymbol{\Lambda}$ and $\boldsymbol{\lambda}$ in the Smoluchowski equation, we choose for convenience to work with our simple approximation. For two binary hydrodynamic interactions this approximation matches correctly the leading orders in the far- and near-field asymptotic limits. We believe that more accurate approximations in the transient domain (moderately large R) will not change significantly the solutions that we have found.

APPENDIX B: POLYNOMIAL CLOSURE

In this appendix we derive a simple closure relation for the fourth order moment $\boldsymbol{M}^{[4]}$; i.e., we express $\boldsymbol{M}^{[4]}$ in terms of the second-order moment $\boldsymbol{m}$ and possibly also of the symmetrized velocity gradient $\boldsymbol{D}$. We follow the strategy introduced in [32,33].

After renormalizing the distribution function $g(\boldsymbol{R})$, we look for a closure relation in the form

$$\boldsymbol{M}^{[4]}(\boldsymbol{m},\boldsymbol{D}) = \mathrm{tr}(\boldsymbol{m})\boldsymbol{W}(\boldsymbol{M},\boldsymbol{D}),$$

where $\boldsymbol{W}$ depends only on the normalized second-order tensor

$$\boldsymbol{M} = \frac{1}{\mathrm{tr}(\boldsymbol{m})}\boldsymbol{m},$$

which has unit trace.

Now, we proceed as follows: First, we select properties of $\boldsymbol{M}^{[4]}$ that we require to be preserved in the closure. Second, we construct functions $\boldsymbol{W}$ of m satisfying the properties.

The properties that we require from $\boldsymbol{W}$ are the following.

(a) Frame indifference: the function $\boldsymbol{W}(\boldsymbol{M},\boldsymbol{D})$ should preserve its form in any coordinate system.

(b) Symmetry: the tensor $W_{\alpha\beta\gamma\delta}$ must be symmetric with respect to permutation of any two indices.

(c) Normalization: $W_{\alpha\alpha\beta\gamma}=M_{\beta\gamma}$.

(d) Boundedness:

(i) Upper boundary:

$$\boldsymbol{W}_{\alpha\beta\gamma\delta} \leqslant 1, \quad \text{for any } \alpha,\beta,\gamma,\delta.$$

(ii) Lower boundary:

$$\boldsymbol{W} \geqslant \boldsymbol{M}\boldsymbol{M},$$

which essentially means that the quadratic form $B(\boldsymbol{q}) = \boldsymbol{q}:(\boldsymbol{W}-\boldsymbol{M}\boldsymbol{M}):\boldsymbol{q}$, defined on 3×3 matrices $\boldsymbol{q}$, is positive definite—i.e., $B(\boldsymbol{q})>0$, for any $\boldsymbol{q}$. This inequality is a consequence of the following relation:

$$B(\boldsymbol{q}) = \langle[\boldsymbol{q}:(\boldsymbol{n}-\langle\boldsymbol{n}\rangle)]^2\rangle,$$

where $\langle\bullet\rangle$ stands for averaging over angle variables: $\langle\bullet\rangle = (4\pi)^{-1}\int \mathrm{d}\boldsymbol{n}\bullet g$. Due to symmetries with respect to index permutations, a more general inequality is valid:

$$\boldsymbol{W} - S_4(\boldsymbol{M}\boldsymbol{M}) \geqslant 0, \tag{B1}$$

where S_4 denotes a symmetrization operator as defined by Eq. (31).

Now, we want to construct $\boldsymbol{W}(\boldsymbol{M})$ satisfying the above properties. To begin with, we assume that the fourth-order tensor $\boldsymbol{W}$ depends only on the second-order tensor $\boldsymbol{M}$ (i.e., we assume that $\boldsymbol{W}$ does not depend explicitly on $\boldsymbol{D}$). This assumption is equivalent to the hypothesis about the *orthotropic* character of a closure relation [32]. Since $\mathrm{tr}\,\boldsymbol{M}$ represents a normalization of the function g in a space of angle variables, the normalized tensor $\boldsymbol{W}$ does not depend on $\mathrm{tr}\,\boldsymbol{M}$ but rather on its traceless part $\mathring{\boldsymbol{M}}=\boldsymbol{M}-1/3\boldsymbol{\delta}$. The tensor $\mathring{\boldsymbol{M}}$ can also be interpreted as a nonequilibrium perturbation of the tensor $\boldsymbol{M}$ [i.e., $\mathring{\boldsymbol{M}}=\boldsymbol{M}-\boldsymbol{M}_{\mathrm{eq}}$, where $\boldsymbol{M}_{\mathrm{eq}}=(1/3)\boldsymbol{\delta}$]. A restriction in the polynomial order in $\mathring{\boldsymbol{M}}$ has then physical interpretation of the restriction to states that are not too far from equilibrium.

Any fourth-order tensor constructed from the second-order tensor $\mathring{\boldsymbol{M}}$ and satisfying the properties (a) and (b) can be written in the form

$$\begin{aligned}\boldsymbol{W} = S_4\{&a_1\boldsymbol{\delta}\boldsymbol{\delta} + a_2\boldsymbol{\delta}\mathring{\boldsymbol{M}} + a_3\boldsymbol{\delta}\mathring{\boldsymbol{M}}\cdot\mathring{\boldsymbol{M}} + a_4\mathring{\boldsymbol{M}}\mathring{\boldsymbol{M}} + a_5\mathring{\boldsymbol{M}}(\mathring{\boldsymbol{M}}\cdot\mathring{\boldsymbol{M}})\\ &+ a_6(\mathring{\boldsymbol{M}}\cdot\mathring{\boldsymbol{M}})(\mathring{\boldsymbol{M}}\cdot\mathring{\boldsymbol{M}})\},\end{aligned} \tag{B2}$$

where the scalar coefficients a_i, $i=1,\ldots,6$ are functions of two invariants: $I_2=\mathrm{tr}(\mathring{\boldsymbol{M}}\cdot\mathring{\boldsymbol{M}})$, $I_3=\mathrm{tr}(\mathring{\boldsymbol{M}}\cdot\mathring{\boldsymbol{M}}\cdot\mathring{\boldsymbol{M}})$.

Condition (b) leaves only three functions (among six functions $a_i, i=1,\ldots,6$) to be linearly independent. The relations determining the first three coefficients are

$$a_1 = \frac{1}{5} + \frac{2}{35}I_2a_4 - \frac{1}{15}I_3a_5 + \frac{2}{35}I_2^2a_6,$$

$$a_2 = \frac{6}{7} - \frac{2}{7}I_2a_5 - \frac{4}{21}I_3a_6,$$

$$a_3 = -\frac{4}{7}(a_4 + I_2a_6). \tag{B3}$$

The remaining coefficients a_4, a_5, and a_6 will be now specified by discussing particular flow regimes.

First, we note that the closure expressions (B2) and (B3) are consistent with the equilibrium solution $\mathring{\boldsymbol{M}}=0$, $\boldsymbol{W} = 4/5S_4(\boldsymbol{\delta}\boldsymbol{\delta})$ by construction (we assume here that all the functions $a_i, i=1,\ldots,6$, are not singular).

In the system of coordinates where $\boldsymbol{M}$ is diagonal, $M_{\alpha\beta} = \delta_{\alpha\beta}c_\alpha$, the axial symmetry of flow means that two among three eigenvalues c_i are equal. We assume that the directions of the eigenvectors of $\boldsymbol{D}$ coincide with the directions of the eigenvectors of $\boldsymbol{M}$. At least one or two eigenvectors related to the eigenvalues a_i are parallel to the directions of the flow elongation. In the limit of strong flows, $\dot{\gamma}\to\infty$, the corresponding eigenvalues become zero. Thus, we can consider two limiting cases: one with two zero eigenvalues and the other with one zero eigenvalue. The first case corresponds to the uniaxial compression flow (squeezing flow) and the second to the uniaxial elongation (biaxial compression) flow. Due to the rotational invariance, we can combine these flows with any kind of homogeneous rotation. Without loss of generality, we can choose for the first case $c_1=1$, $c_{2,3}=0$ and for the second case $c_1=0$, $c_2=1/2$, and $c_3=1/2$. The elements of $\boldsymbol{W}$ become, in the first case, $W_{1111}=1$, $W_{2222}=0$, and $W_{3333}=0$, and in the second case, $W_{1111}=0$, $W_{2222}=3/8$, and $W_{3333}=3/8$. We note that the remaining components depend on these three components due to the symmetry and the normalization properties (a) and (b). We shall limit ourselves to the case when the coefficients a_4, a_5, and a_6 are constants—i.e., independent of R and of the invariants I_2, I_3. Substituting the data for the two strong flows into expression (B2) we find one parametric set of solutions:

$$a_4 = \frac{4}{3} - \frac{1}{18}a_6,$$

$$a_5 = -1 - \frac{1}{6}a_6.$$

Our choice for coefficient choice is $a_6=6$ which leads to the solution

$$a_4 = 1, \quad a_5 = -2, \quad a_6 = 6. \tag{B4}$$

This choice of a_6 is dictated by the restriction (d ii) (which implies $a_6>0$) and by requiring that the part of the closure (34), including terms up to the second polynomial order with respect to $\mathring{\boldsymbol{M}}$ (the case $a_5=0$ and $a_6=0$), represent also a valid closure relation. By a valid closure we mean a closure that satisfies the requirements (a)–(d), matches the near-equilibrium solution, and matches one strong flow limit: namely, the uniaxial compression flow.

APPENDIX C: FINITE-ELEMENT METHOD FOR SOLVING THE MS EQUATION

In this appendix we discuss the finite-element method that we use to solve Eqs. (32)–(34). The first problem that we have to tackle is the unboundedness of the domain of R. We solve it by introducing a new variable x by $R\to x=1/R$. The variable x has now a bounded domain $0\leqslant x\leqslant 1/2$. Under the transformation $R\to x=1/R$, Eq. (33) becomes the following partial differential equation:

$$\begin{aligned}\frac{\partial \boldsymbol{m}}{\partial t} = \mathrm{Pe}\Bigg\{ & \boldsymbol{\omega}\cdot\boldsymbol{m} - \boldsymbol{m}\cdot\boldsymbol{\omega} - x^2\frac{\partial}{\partial x}x^{-1}R(\mu_1-1)\boldsymbol{M}^{[4]}\mathbin{:}\boldsymbol{D} \\ & + (1-\mu_2)(\boldsymbol{D}\cdot\boldsymbol{m} + \boldsymbol{m}\cdot\boldsymbol{D} - 2\boldsymbol{M}^{[4]}\mathbin{:}\boldsymbol{D})\Bigg\} + x^2\frac{\partial}{\partial x}\sigma_1 g_{\mathrm{eq}} \\ & \times\frac{\partial}{\partial x}\frac{\boldsymbol{m}}{\hat{g}_{\mathrm{eq}}} - 6\sigma_2 x^2\mathring{\boldsymbol{m}}.\end{aligned} \tag{C1}$$

In order to solve it, we introduce the finite-element approximation of $\boldsymbol{m}(x)$:

$$\boldsymbol{m}(x) = \boldsymbol{m}_{\mathrm{eq}}(x) + g_{\mathrm{eq}}\sum_{n=1}^{N} e_n(x)\boldsymbol{m}_n, \tag{C2}$$

where the functions e_n represent a fixed set of finite elements.

The second problem that we have to face is the nonpolynomial nonlinearity appearing in the closure $\boldsymbol{M}^{[4]}(\boldsymbol{m},x)$. We solve this problem by turning to the *group finite-element method* [30] which suggests to expand the nonlinear term $\boldsymbol{M}^{[4]}(\boldsymbol{m},x)$ in the finite elements as follows:

$$\boldsymbol{M}^{[4]}(\boldsymbol{m},x) = \boldsymbol{M}^{[4]}_{\mathrm{eq}}(x) + \sum_{n=1}^{N} e_n(x)\hat{\boldsymbol{M}}^{[4]}_n, \tag{C3}$$

where $\hat{\boldsymbol{M}}^{[4]}_n(\boldsymbol{m},x)=\boldsymbol{M}^{[4]}(\boldsymbol{m}_n,x_n)/g_{\mathrm{eq}}(x_n)$ and $\boldsymbol{M}^{[4]}_{\mathrm{eq}}(x)$ is the value of the function $\boldsymbol{M}^{[4]}(\boldsymbol{m},x)$ at equilibrium, $\boldsymbol{M}^{[4]}_{\mathrm{eq}}(x)=\boldsymbol{M}^{[4]}(\boldsymbol{m}_{\mathrm{eq}},x)$, or, explicitly,

$$\boldsymbol{M}^{[4]}_{\mathrm{eq}}(x) = \frac{1}{5}\hat{g}_{\mathrm{eq}}(x)S_4(\delta\delta).$$

In the rest of the calculations we follow the standard Galerkin method with averaging given by $\langle\bullet\rangle_{\mathrm{eq}}=\int_0^{1/2}\mathrm{d}\boldsymbol{x}g_{\mathrm{eq}}\cdot$; g_{eq} is the equilibrium correlation function. We arrive at the following system of equations:

$$\begin{aligned}\sum_k u_{nk}[\dot{\boldsymbol{m}}_k - \mathrm{Pe}(\omega\cdot\boldsymbol{m}_k - \boldsymbol{m}_k\cdot\omega)] & \\ = \mathrm{Pe}h_n\boldsymbol{D} + \mathrm{Pe}\Bigg[\sum_k q_{nk}\boldsymbol{w}_k\mathbin{:}\boldsymbol{D} & + \sum_k r_{nk}(\boldsymbol{D}\cdot\boldsymbol{m}_k + \boldsymbol{m}_k\cdot\boldsymbol{D} \\ - 2\boldsymbol{w}_k\mathbin{:}\boldsymbol{D})\Bigg] & - \sum_k \Omega_{nk}\boldsymbol{m}_k - \sum_k \Gamma_{nk}\mathring{\boldsymbol{m}}_k,\end{aligned} \tag{C4}$$

with the coefficients

$$\begin{aligned}u_{nk} &= \langle e_n e_k\rangle_{\mathrm{eq}}, \\ q_{nk} &= \left\langle\left(2e_n + x\frac{\partial e_n}{\partial x}\right)(\mu_1-1)e_k\right\rangle_{\mathrm{eq}}, \\ r_{nk} &= \langle e_n e_k(1-\mu_2)\rangle_{\mathrm{eq}}, \\ \Omega_{nk} &= \left\langle x^2\sigma_1\left(2e_n + x\frac{\partial e_n}{\partial x}\right)\left(2e_k + x\frac{\partial e_k}{\partial x}\right)\right\rangle_{\mathrm{eq}}, \\ \Gamma_{nk} &= 6\langle e_n x^2\sigma_2 e_k\rangle_{\mathrm{eq}}, \\ h_n &= \frac{2}{15}\left\langle x^{-2}e_n\left[3(\mu_1-\mu_2) - x\frac{\partial\mu_1}{\partial x} - x\frac{\partial U_{\mathrm{nl}}}{\partial x}(1-\mu_1)\right]\right\rangle_{\mathrm{eq}} \\ &\quad + \frac{4}{15}[g_{\mathrm{eq}}(\mu_1-1)e_n]|_{x=1/2}.\end{aligned} \tag{C5}$$

The boundary condition (6) is accounted for by requiring that all finite-element functions e_k take zero value at the boundary $x=0$—i.e., $e_k(0)=0$, $k=0,\ldots,N$. The second boundary condition (9) is a *natural* boundary condition for the partial differential equation (C1). It is incorporated via boundary terms emerging in by part integrations [the last term in the expression for h_n in Eq. (C5)]. The matrices $\boldsymbol{\Omega}$ and Γ are symmetric and positive definite due to our choice of integration weights e_n and finite-element functions $g_{\mathrm{eq}}e_k$. Consequently, it is the choice of the finite-element approximation (C2) and of the integration weights that provides us with the required dissipative properties of the finite-element form of the irreversible part of the time evolution equations.

In our subsequent calculations we choose the finite-element functions e_n to be a standard linear elements [30] which are associated with the partition of the interval $[0,1/2]$ by a set of points $x_0 < x_1 < \cdots < x_N$, where $x_0 = 0$ and $x_N = 1/2$.

After solving Eq. (C1), we compute the stress tensor which, in the the finite-element approximation, becomes

$$\sigma = -\left(1 + \frac{5}{2}\phi\right)\boldsymbol{D} + \frac{405}{4}\frac{\phi^2}{\mathrm{Pe}}\sum_{n=0}^{N} h_n \mathring{\boldsymbol{m}}_n, \tag{C6}$$

where h_n are taken from Eq. (C5).

To solve the linear response equation (38) we use the linearized version of the same finite-element method. With the finite-element approximation

$$f = \sum_n e_n(x) f_n, \tag{C7}$$

we are led to the following algebraic equation:

$$(\Omega_{nk} + \Gamma_{nk} + i\omega L_{nk}) f_k = h_n, \tag{C8}$$

with the matrices Ω_{ij}, Γ_{ij}, and L_{ij} and the vector h given in Eqs. (C5). We note that Eq. (C8) has to be solved for real and imaginary parts of the coefficients f_n.

[1] B. U. Felderhof, Physica A **147**, 203 (1987); **146**, 417 (1987); J. Fluid Mech. **225**, 177 (1991).

[2] G. Wilemski, J. Stat. Phys. **14**, 153 (1976).

[3] N. Phan-Thien, J. Rheol. **39**, 679 (1995).

[4] V. G. Kolli, E. J. Pollaf, and F. Gadala-Maria, J. Rheol. **46**, 321 (2002); Jae-Hyun So, Seung-Man Yang, and Jae Chun Hyun, Chem. Eng. Sci. **56**, 2967 (2001); N. Ohl and W. Gleissle, J. Rheol. **37**, 381 (1993); F. Gadala-Maria and Andreas Acrivos, *ibid.* **26**, 799 (1980).

[5] J. F. Brady, Chem. Eng. Sci. **56**, 2921 (2001).

[6] J. Bławzdziewicz and G. Szamel, Phys. Rev. E **48**, 4632 (1993).

[7] S. Hess, Phys. Rev. A **22**, 2844 (1980).

[8] H.-M. Koo, Phys. Rev. E **47**, 1685 (1993).

[9] J. K. G. Dhont, J. Fluid Mech. **204**, 421 (1989).

[10] S. Kim and S. J. Karrilla, *Microhydrodynamics. Principle and Selected Application* (Butterworth-Heinmann, Boston, 1991).

[11] J. C. Rainwater and S. Hess, Physica A **118**, 371 (1983).

[12] R. A. Lionberger and W. B. Russel, J. Rheol. **38**, 1885 (1994).

[13] W. B. Russel and A. P. Gast, J. Chem. Phys. **84**, 1815 (1986).

[14] R. B. Bird, C. F. Curtiss, R. Armstrong, and O. Hassager, *Kinetic Theory, Vol. 2 of Dynamics of Polymeric Liquids* (John Wiley & Sons, New York, 1987).

[15] V. B. Zmievski, I. V. Karlin, and M. Deville, Physica A **275**, 152 (2000).

[16] M. v. Smoluchowski, Ann. Phys. **48**, 1103 (1915).

[17] G. K. Batchelor, J. Fluid Mech. **83**, 97 (1977).

[18] G. K. Batchelor, J. Fluid Mech. **74**, 1 (1976).

[19] Peter Constantin (private communication).

[20] G. K. Batchelor and J. T. Green, J. Fluid Mech. **56**, 401 (1972).

[21] R. Schmitz and B. U. Felderhof, Physica A **116**, 163 (1982).

[22] R. B. Jones and R. Schmitz, Physica A **149**, 373 (1988).

[23] H. J. H. Clercx and P. P. J. M. Schram, Physica A **171**, 293 (1991); **171**, 325 (1991).

[24] M. Grmela, Phys. Lett. **111**, 41 (1985).

[25] M. Grmela, Contemp. Math. **28**, 125 (1984); Physica D **21**, 179 (1986); in *Rheological Modelling: Thermodynamics and Statistical Approaches*, edited by J. Casas-Vazquez and D. Jou, Lecture Notes in Physics, Vol. 381 (Springer-Verlag, Berlin, 1991), pp. 126–158; M. Grmela and H. G. Oettinger, Phys. Rev. E **56**, 6620 (1997); H. C. Oettinger and M. Grmela, *ibid.* **56**, 6633 (1997).

[26] M. Grmela, Physica A **309**, 304 (2002).

[27] A. Einstein, Ann. Phys. **19**, 289 (1906); **34**, 591 (1906).

[28] G. K. Batchelor and J. T. Green, J. Fluid Mech. **56**, 375 (1972).

[29] D. E. Erlick, Aust. J. Phys. **15**, 283 (1962).

[30] P. K. Kythe, *An Introduction to Linear and Nonlinear Finite Element Analysis: A Computational Approach* (Birkhauser, Boston, 2004).

[31] D. J. Jefrey and Y. Onishi, J. Fluid Mech. **139**, 261 (1984).

[32] J. S. Sintra and C. L. Tucher III, J. Rheol. **39**, 73 (1995).

[33] Du Hwang Chung and Tai Hun Kwon, J. Rheol. **46**, 169 (2002); M. Grosso, P. L. Maffettone, and F. Dupret, Rheol. Acta **39**, 301 (2000).